Revista Brasileira de Farmacognosia 29 (2019) 401–424

Brazilian Journal of Pharmacognosy
REVISTA BRASILEIRA DE FARMACOGNOSIA
www.elsevier.com/locate/bjp

Original Article

"Arnicas" from Brazil: comparative analysis among ten species

Amanda Ellen de Athayde [a], Everton Richetti [b], Josiane Wolff [b], Makeli Garibotti Lusa [b], Maique Weber Biavatti [a,*]

[a] Departamento de Ciências Farmacêuticas, Centro de Ciências da Saúde, Universidade Federal de Santa Catarina, Florianópolis, SC, Brazil
[b] Departamento de Botânica, Centro de Ciências Biológicas, Universidade Federal de Santa Catarina, Florianópolis, SC, Brazil

ARTICLE INFO

Article history:
Received 26 October 2018
Accepted 6 February 2019
Available online 23 March 2019

Keywords:
Arnica
Morphoanatomy
Phytochemical review
Quality control
Asteraceae
Ethnopharmacology

ABSTRACT

The "arnicas" found in Brazil are examples of different species of the family Asteraceae used in popular medicine for its attributed anti-inflammatory action. Among the species known and used as "arnica" we selected: *Calea uniflora* Less., *Chaptalia nutans* (L.) Polák, *Lychnophora ericoides* Mart., *Lychnophora pinaster* Mart., *Lychnophora salicifolia* Mart., *Lychnophora diamantinana* Coile & S.B.Jones, *Porophyllum ruderale* (Jacq.) Cass., *Pseudobrickellia brasiliensis* (Spreng.) R.M.King & H.Rob., *Sphagneticola trilobata* (L.) Pruski, and *Solidago chilensis* Meyen, due to their extensive use. This research provides new information on leaf morphology and anatomy and on chemistry of the major metabolites found in these species through histochemical tests and phytochemical review. The results revealed anatomical characters for the differentiation and quality control of the vegetal drugs, being these: distinctive epidermal attachments, epidermis cells, parenchymal cells of the mesophyll, vascular bundles, midvein patterns and secretory structures of exudation of secondary metabolites. The review of chemical profiles showed differences in the chemical composition of the species, as different skeletons of sesquiterpene lactones in the species evaluated in addition to other chemical classes such as terpenes, flavonoids, chromenes and phenolic acids derivate. Based on the results obtained in this work it is important to emphasize that the information about the ten species of arnica generate subsidies for differentiation and identification of characteristic markers and for the diagnosis of the species and it can be applied in the "arnicas" quality control.

Introduction

Brazil has a huge plant diversity and wide sociodiversity. For this reason, the country presents great potential for the development of phytotherapy and correlated sciences. The popular use of medicinal plants in Brazil is a process of production and reproduction of varied knowledge and practices originated in different cultures, resulted from the social interaction among several groups that composes, in this case, the Brazilian culture (European, African and indigenous communities, among many other cultural groups) (Sales et al., 2015).

The European immigrants that arrived to work mainly in coffee plantation in Brazil (19–20th centuries) could not find here the European medicinal plants, such as the very well known *Arnica montana*, used as topical anti-inflammatory. To meet the need for this species, immigrants began to look for other species that could provide the same therapeutic effects; this selection was anecdotally based on morphological and sensorial characters that could resemble the true arnica (*A. montana*). Over the years, the combination of the European heritage with the miscegenation with other ethnic and culture groups, led to a selection of several plants named popularly as "arnica", arising from some resemblance to the *A. montana* (Semir et al., 2011). Similar processes occurred also in other countries, for example in Mexico is common the use of *Heterotheca inuloides* Cass., Asteraceae, known as "arnica-mexicana" (Rodríguez-Chávez et al., 2017). According to Obón et al. (2012), in the Iberic peninsula and Balearic Islands, about 32 species are known as "arnica" belong to six botanical families. A total of 24 species are Asteraceae, belonging to eight tribes: *Anthemideae* Cass. (*Achillea ageratum* L.); *Astereae* Cass. (*Conyza bonariensis* (L.) Cronquist); *Cardueae* Cass. (*Centaurea granatensis* Boiss. ex DC.); *Cichorieae* Lam. & DC. (*Andryala integrifolia* L., *A. ragusina* L., *Crepis paludosa* (L.) Moench, *C. vesicaria* L. subsp. *taraxacifolia* (Thuill.) Thell., and *Hieracium* sp.); *Doroniceae* Panero (*Doronicum carpetanum* Boiss. & Reut. ex Willk. & Lange, *D. grandiflorum* Lam. and *D. pardalianches* L.); *Inulaeae* Cass. (*Chiliadenus glutinosus* (L.) Fourr., *Dittrichia viscosa* (L.) Greuter, *Inula britannica* L., *I. helenioides* DC., *I. helvetica* Grauer, *I. montana* L., *I. salicina* L., *Pallensis spinosa* (L.) Cass., *Pulicaria odora* (L.) Rchb., and *P. paludosa* Link.); *Madieae* Jeps. (*A. montana* L.). *Senecioneae* Cass. (*Senecio*

* Corresponding author.
E-mail: maique.biavatti@ufsc.br (M.W. Biavatti).

https://doi.org/10.1016/j.bjp.2019.02.006

doronicum (L.) L., *S. jacobaea* L., and *S. pyrenaicus* L.) (Obón et al., 2012).

In this sense, several species can be designated just as "arnica", difficulting the correct determination of the species when they are packaged crushed or powdered. The lack of information on the morphoanatomy of these species together with the lack of established chemical markers of the "arnicas" contributes to the misidentification and therefore to an inefficient quality control of these plant drugs. This fact also compromises the scientific verification of the effectiveness of the use of these several related species. In this cultural aspect of the popular use is not possible to say that the species used in Brazil are forgeries of the original one, because it is not found in the Brazilian territory (there is a wider context of popular use involved that will not be considered in this work).

Thus, this study will provide information about the microanatomical characterization of the most usual "arnicas" in Brazil, defining anatomical markers and comparing their phytochemical composition based on published papers to differentiate these species, namely: *Calea uniflora* Less. (arnica-da-praia), *Chaptalia nutans* (L.) Polák (arnica-língua-de-vaca), *Lychnophora ericoides* Mart. (arnica-da-serra), *Lychnophora diamantinana* Coile & S.B.Jones (arnica-da-serra), *Lychnophora pinaster* (arnica-da-serra) Mart. and *Lychnophora salicifolia* Mart. (arnica-falsa, arnica-do-cerrado), *Porophyllum ruderale* (Jacq.) Cass. (arnica-paulista, arnica-da-praia), *Pseudobrickellia brasiliensis* (Spreng.) R.M.King & H.Rob. (arnica-do-campo, arnica-do-mato), *Solidago chilensis* Meyen (arnica-brasileira, arnica-do-campo) and *Sphagneticola trilobata* (L.) Pruski (arnica-do-mato).

The species *L. ericoides* and *L. pinaster* are very similar species and sometimes the separation between them is difficult. Although the species are considered by some authors as synonyms, in this work we are considering as different species. The characteristics used to identify *L. ericoides* and *L. pinaster* are described in the Supplementary Material.

Species of *Senecio* ("pseudo-arnica"), Asteraceae, are also used as arnica but were not included in this work because its medicinal use should be discouraged due to the presence of the toxic pyrrolizidine alkaloids in this genus (Sandini et al., 2013).

Material and methods

Plant material used in this study

The plant material analyzed was collected in Santa Catarina State (SC) and Minas Gerais State (MG), Brazil. The samples were obtained in field or from exsiccates deposited in the FLOR Herbarium of the Federal University of Santa Catarina and from herborized material provided by Benoit Loeuille. *A. montana* was obtained of commercial sample in Barcelona, Spain. Whenever possible, the leaves used in this study were collected from triplicate of three different populations. Voucher number of the species can be found in Table 1.

Table 1
List of "arnica" species used in this study.

Species	Voucher	Herbarium
Arnica montana[c]		–
Calea uniflora	FLOR63637	FLOR[a]
Chaptalia nutans	FLOR63636	FLOR[a]
Lychnophora diamantinana	Loeuille et al. 530	SPF[b]
Lychnophora ericoides	Pirani 1726	SPF[b]
Lychnophora pinaster	Mello Silva 1389	SPF[b]
Lychnophora salicifolia	Mello Silva 3000	SPF[b]
Porophyllum ruderale	FLOR63635	FLOR[a]
Pseudobrickellia brasiliensis	FLOR46719	FLOR[a]
Solidago chilensis	FLOR63638	FLOR[a]
Sphagneticola trilobata	FLOR63634	FLOR[a]

[a] FLOR Herbarium of the Federal University of Santa Catarina.
[b] SPF Herbarium of University of São Paulo.
[c] Commercial sample identified as described in the Brazilian Pharmacopoeia 5th edition (Farmacopeia Brasileira, 2010).

Anatomical analysis

For morphoanatomical analysis, leaves from three distinct populations ($n = 3$) of species collected in field were fixed in FAA solution (70% ethanol, 40% formalin, glacial acetic acid) under vacuum conditions to remove air from the tissues (Johansen, 1940). Next, the materials were dehydrated in a growing series of ethanol (30%, 50%, 70%) and stored in 70% ethanol. The herborized material was hydrated using a Smith and Smith (1942) modified method (for this process was added one drop of detergent). Afterwards, the median region of the leaf (medium third) was selected and the samples were infiltrated in PEG 1500. The samples were then cross-sectioned with a variation between 15 μm and 35 μm thickness using a rotary microtome, model RM 2125 RT Leica Microsystem, Nussoch, Germany. To prepare the permanent histological slides, the cross-sections were stained with 0.05% Toluidine Blue in citrate-phosphate buffer, pH 4.5 (Sakai, 1973) and affixed to the slides using synthetic Canada balm. For visualization of the epidermis in frontal view, dissociation of the epidermis was performed (Johansen, 1940).

Histochemical reactions

Histochemical reactions were chosen based on the chemical classes of higher occurrence in the Asteraceae family and were performed on material embedded in PEG 1500. The following chemical reactions were carried out: Sudan IV (Jensen, 1962) for lipophilic compounds; sulphuric acid (Geissman and Griffin, 1971) for sesquiterpene lactones; ferric chloride 3% (Johansen, 1940) for phenolic compounds; and Ruthenium Red for pectic compounds. The sections were examined immediately after each reaction. Control sections were performed simultaneous to the histochemical tests, in accordance with standard procedure.

Images capturing

All the histological slides, including that of histochemical reactions, were observed of the Leica® Microscope Model DM2500 coupled to the Leica® Model DFC29 video camera. To capture the images with sulphuric acid was used an Olympus® microscope (model CX21FS1) by attaching a digital camera (Olympus T110) to eyepiece. To verify the crystals, the histological slides were analyzed under polarized light using the Olympus BX50 microscope coupled to the Olympus DP 73 camera, through which the images were captured.

Scanning electron microscopy (SEM)

To perform this procedure, the plants were fixed using FAA solution and incubated for a period of 24 h (Johansen, 1940). After that, the samples were dehydrated in a growing series of ethanol (30%, 50%, 70%, 80%, 90% and 100%) was performed 20 min each. Subsequently, the material was dried using the CO_2-critical method and, finally, the samples were metalized with gold for analysis by SEM (Fernandes et al., 2016) and analyzed by SEM with the JEOL JSM-6390LV Scanning Electron Microscope.

Phytochemical review

Phytochemical investigations of "arnicas" species was performed using the Reaxys, Scifinder, Pubmed, Sciencedirect, Google Scholar and Tropicos databases. The data obtained was plotted in comparative table, correlating the "arnica" species with their respective metabolites according to the literature. Phytochemical survey was carried out from March 2017 to July 2018. There was no minimum date for inclusion of the data, so all data was included until the year 2018.

Results

Micromorphological characterization

All the samples of leaves of the species analyzed are illustrated in Figs. 1(A-J), 2(A-F), 3(A-I), 4(A-J′), 5(A-G′), 6(A-G), 7(A-H), 8(A-H″), 9(A-J), 10(A-J′), 11(A-G) and the aim characteristics are summarized in Figs. 12–14. The complete morphoanatomical description of these samples follows below.

Middle vein

Initially the middle vein (MV), in cross section, was evaluated. The species *C. uniflora*, *C. nutans* and *S. chilensis* presented the MV with a biconvex form, with the abaxial region more prominent (Fig. 1A, B, J). The species *L. diamantinana*, *L. ericoides*, *L. pinaster* and *L. salicifolia* presented adaxial surface with central depression and abaxial face with rounded projection (Fig. 1C–F). For *P. brasiliensis* it was observed a little defined MV, without great differentiation of the strata of parenchyma, and is not possible to discuss clearly them format (Fig. 1H). The species *P. ruderale* and *S. trilobata* presented, respectively, a convex and concave-convex middle vein form (Fig. 1G, I).

The epidermal cells, for all species, present uniseriate form and covered by cuticle. Adjacent to the epidermis of the *C. uniflora* and *C. nutans* was observed an angular collenchyma turned to adaxial face (Fig. 1A and B). For the *S. trilobata* and *S. chilensis* was found angular collenchyma in both surfaces (Fig. 1I–J). *Lychnophora* species presented a lot of collenchyma cells in both surfaces, being them lamellar collenchyma to *L. ericoides* and sclerehydeified cells or fibers associated with the phloem (Fig. 1C–F). *P. ruderale*, showed a stratum of angular collenchyma in both faces with the extension of the sheath of the collenchyma bundle (Fig. 1G).

Internal secretory structures were observed close to the vascular bundles, dispersed in the parenchyma of the MV. The taxa *C. uniflora* and *S. trilobata* presented two secretory cavities inserted in the parenchyma facing the abaxial surface, close to the phloem, and a secretory cavity just above the xylem, turned to adaxial surface (Fig. 1A and I). *S. chilensis* presented a secretory cavity turned to abaxial face, inserted below the phloem of the MV of the leaf (Fig. 1J). *S. trilobata* presented three secretory cavities, two turned to abaxial face, below the phloem and one facing the adaxial surface, above the xylem; the other species did not present cavities in the MV region (Fig. 1I).

The vascular bundles in transversal section present in the middle vein (MV) of *C. uniflora* is organized in open arch form (Fig. 1A and E, respectively). *C. nutans* presents a relatively cilindric vascular bundle (Fig. 1B). The species of *Lychnophora* presented three free bundles with cilindric form (Fig. 1C, D, F). *P. ruderale* presents small and straight vascular pattern with extension of the bundle sheath (Fig. 1G). *P. brasiliensis* does not present specific delimitations, with vascular bundles distributed throughout the mesophyll (Fig. 1H). *S. chilensis* presented a cord format vascular system and, the taxon

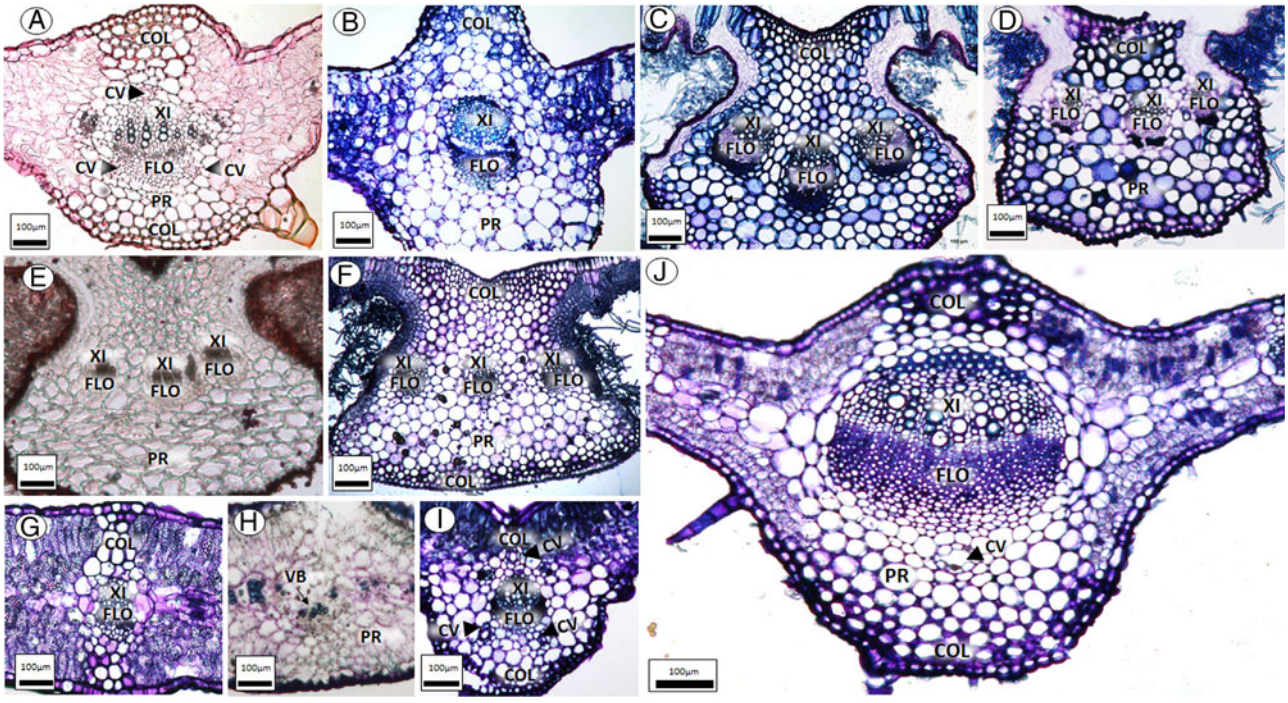

Fig. 1. Middle vein (MV) in cross-sections of leaves fully expanded of "arnicas". A–J. Light microscopy. A. *Calea uniflora*; B. *Chaptalia nutans*; C. *Lychnophora diamantinana*; D. *Lychnophora ericoides*; E. *Lychnophora pinaster*; F. *Lychnophora salicifolia*; G. *Porophyllum ruderale*; H. *Pseudobrickellia brasiliensis*; I. *Sphagneticola trilobata*; J. *Solidago chilensis*. A. Staining with ruthenium red; B–D, F–J. Staining with toluidine blue; E. Staining with Sudan. Abbreviations: COL, collenchyma; XI, xylem; FLO, phloem; PAR, regular parenchyma; ESC, sclerehydes; CV, internal secretory cavity. A, J, I. presence of CV; E. presence of ESC. C–F. possible sclerenchyma fibers below the phloem. Findings: A, B, J. MV with biconvex form; C, F. adaxial face with central depression and abaxial face with rounded projection to the MV form; H. undefined MV; G. convex MV form; I. concave-convex MV form; A–J. uniseriate epidermal cells, covered by cuticle; A. open arch vascular bundles form; B. cord format vascular bundles form; C–F. three free bundles with cilindric form; G. small and straight vascular pattern with extension of the bundle sheath; H. undefined vascular bundles form; I. cord format vascular bundles form; J. conical and small dimensions vascular bundles form.

Sphagneticola tilobata presented vascular bundles with "conical and small dimensions" (Fig. 1J–I).

Intermediate region of the mesophyll

In the intermediate region of the mesophyll (IR) was observed (a higher concentration of stomata in the abaxial face with anomocytic characteristics for the species *C. uniflora*, *C. nutans*, *P. ruderale*, *P. brasiliensis*, *S. chilensis* and *S. trilobata* (Fig. 2A–F). However, due to the insertion of the stomata in the crypts at *Lychnophora* species, it was not possible to identify the guard cell forms, and it is not possible to classify the stomata in these species.

Through SEM, the level of stomata in relation to the epidermis can be verified, being regular for *C. uniflora*, *C. nutans* and *S. trilobata* (Fig. 3A, B, H); below the epidermis in *L. ericoides*, *P. ruderale* and *P. brasiliensis* (Fig. 3C, F, G); above the epidermis in *L. salicifolia* and *L. pinaster* and *S. chilensis* (Fig. 3D, E, I).

The leaf pattern of the stomata was amphistomatic (stomata on both surfaces) verified in the species *C. uniflora*, *P. ruderale*, *P. brasiliensis*, *S. chilensis* and *S. trilobata* (Fig. 4A, G–D′, I–J′). The

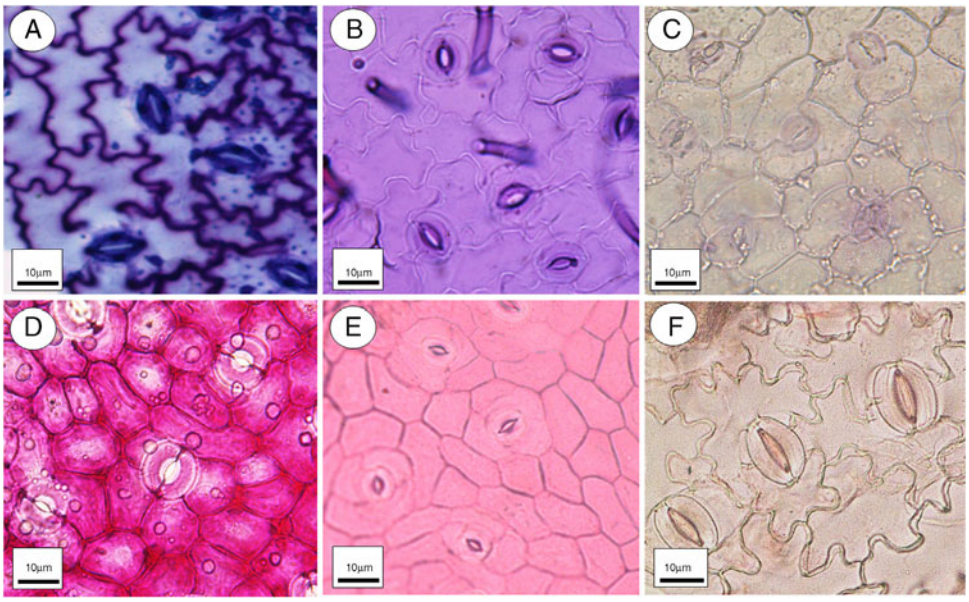

Fig. 2. View of stomata and epidermal cells in abaxial surface of leaves fully expanded of "arnicas". A–F. Light microscopy; A. *Calea uniflora*; B. *Chaptalia nutans*; C. *Porophyllum ruderale*; D. *Pseudobrickellia brasiliensis*; E. *Sphagneticola trilobata*; F. *Solidago chilensis*; A–B. Staining with toluidine blue. C–F. Staining with safranine. Findings: A–F. anomocytic characteristics by stomata.

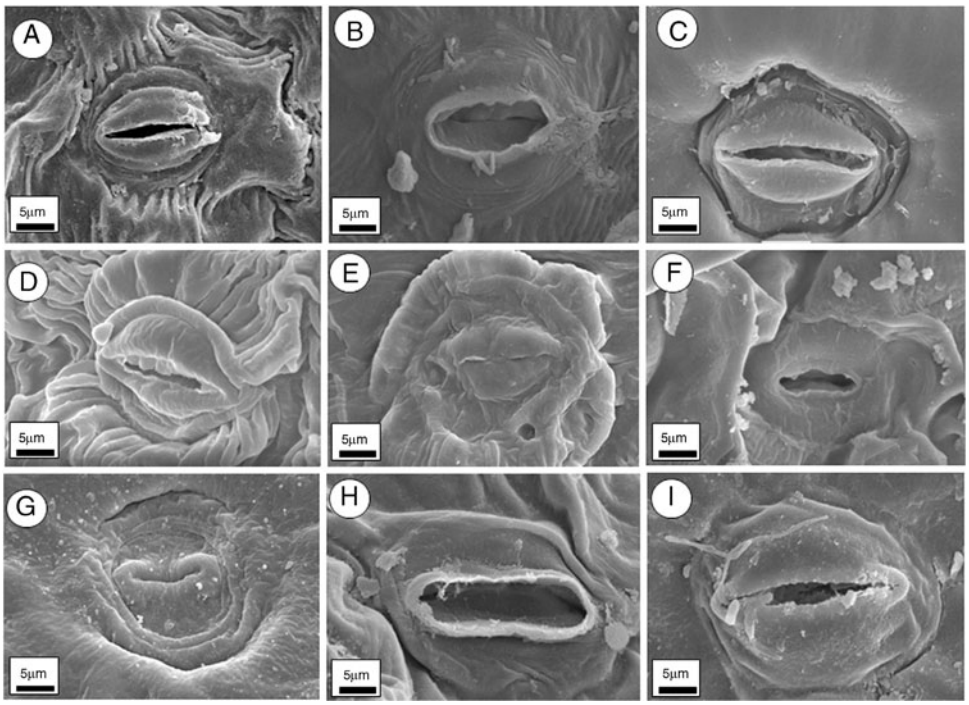

Fig. 3. View of stomata in abaxial surface of leaves fully expanded of "arnicas" by SEM. A. *Calea uniflora*; B. *Chaptalia nutans*; C. *Lychnophora ericoides*; D. *Lychnophora pinaster*; E. *Lychnophora salicifolia*; F. *Porophyllum ruderale*; G. *Pseudobrickellia brasiliensis*; H. *Sphagneticola trilobata*; I. *Solidago chilensis*. Findings: A, B, H. regular level of stomata in relation to the epidermis. C, F–G. below of the epidermis level. D, E, I. above the epidermis level.

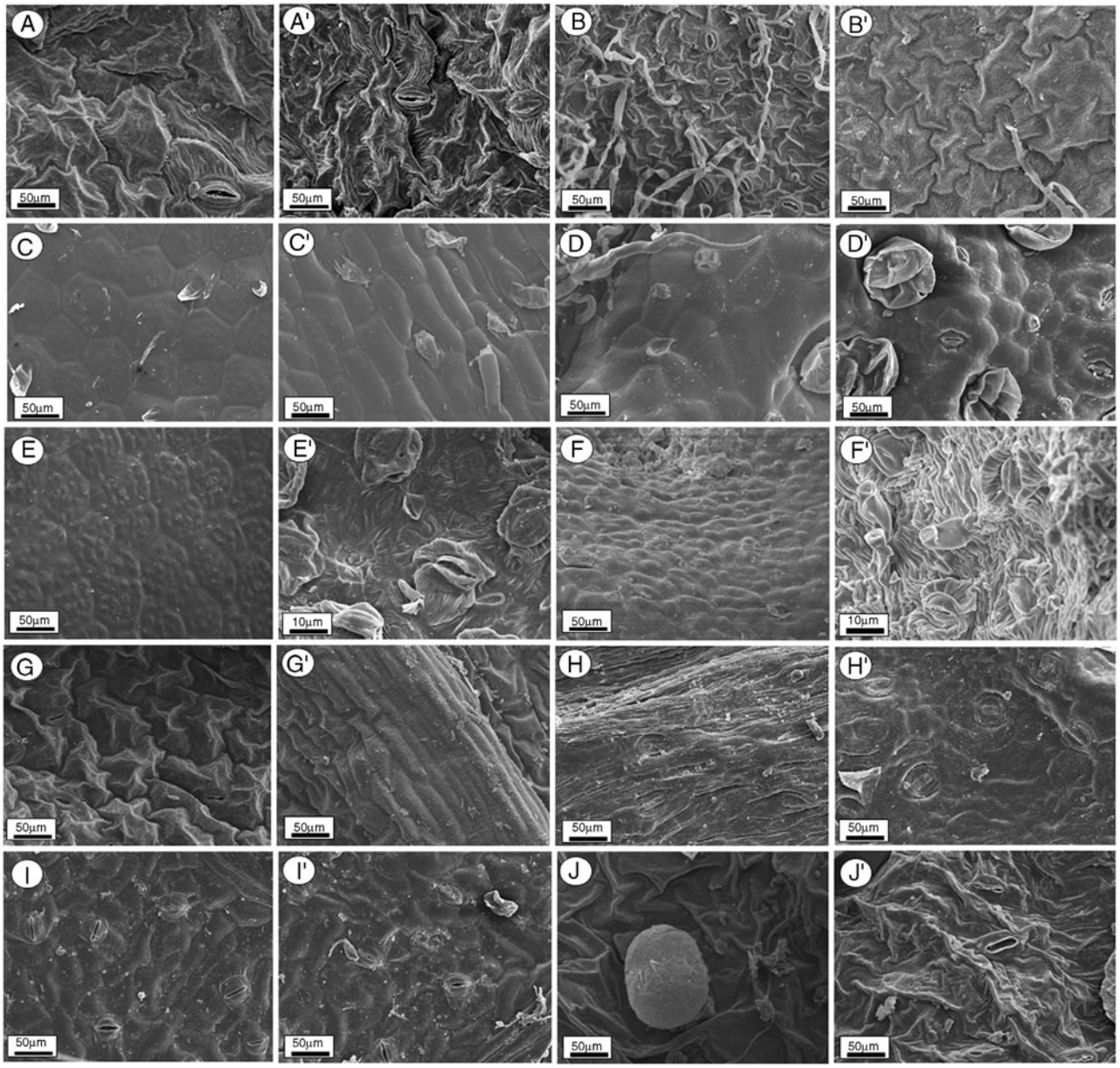

Fig. 4. Epidermis cells (adaxial *vs.* abaxial surface) of leaves fully expanded of "arnicas" by SEM. Adaxial face: A. *Calea uniflora*; B. *Chaptalia nutans*; C. *Lychnophora diamantinana*; D. *Lychnophora ericoides*; E. *Lychnophora pinaster*; F. *Lychnophora salicifolia*; G. *Porophyllum ruderale*; H. *Pseudobrickellia brasiliensis*; I. *Sphagneticola trilobata*; J. *Solidago chilensis*. Abaxial face: A′. *Calea uniflora*; B′. *Chaptalia nutans*; C′. *Lychnophora diamantinana*; D′. *Lychnophora ericoides*; E′. *Lychnophora pinaster*; F′. *Lychnophora salicifolia*; G′. *Porophyllum ruderale*; H′. *Pseudobrickellia brasiliensis*; I′. *Sphagneticola trilobata*; J′. *Solidago chilensis*. Findings: A–J and A′–J′. uniform epidermis of the leaf surface (both faces); A, B, I and A′, B′, I′. sinuous walls of the epidermal cells; G, H, J and G′, H′, J′. straight wall of the epidermal cells; C–F and C′–F′. straight wall of the epidermal cells in the adaxial face (C–F) being more rounded and the abaxial cells (C′–F′) more elongated.

hypostomatic leaf pattern was observed to the *C. nutans*, *L. diamantinana*, *L. ericoides*, *L. pinaster* and *L. salicifolia* (Fig. 4B–F′).

The sinuosity of the epidermal cells showed significant difference for each species. The "arnicas" presented the leaf surface (both faces) with uniform epidermis, whose cells in frontal view presented sinuous walls to the taxons *C. uniflora*, *C. nutans* and *S. trilobata* (Fig. 4A–B′, I–I′). Straight wall was observed for *P. ruderale* (long and straight cells in adaxial face), *P. brasiliensis* (both sides) and *S. chilensis* (both sides) (Fig. 4G–H′, J–J′). For the *Lychnophora* species, the form of the cells was identified as straight, with the cells in the adaxial face being more rounded and the abaxial cells more elongated (Fig. 4C–F and C′–F′).

The presence of glandular (GT) and non-glandular trichomes (NGT) were verified to the *C. uniflora*, *C. nutans* (NGT only), *L. ericoides*, *L. diamantinana*, L pinaster and *L. salicifolia*, *S. chilensis* and *S. trilobata* (Figs. 5A–G′, 6A–G, 6A–H and 7A–H″). The species *P. ruderale* and *P. brasiliensis* presented glabrous leaf. In *C. uniflora*, the GT are inserted in small depression in the epidermis and can be multicellular and bicellular or capitate with unicellular pedicel and globoid head (Figs. 5A and 6A). The *Lychnophora* species evaluated showed GT concentrated on the abaxial face inclosed in crypts (Figs. 5B–E and 6B–E). *S. chilensis* presented multicellular trichomes, plurisseriate and/or capitate with unicellular pedicel with elongated terminal cell (Figs. 5F–F″, 6G). *S. trilobata* presented biseried GT in depression and/or multicellular unisseriate GT with elongated terminal cell (Figs. 5G, 6F).

Multicellular (5–8 cells) and unisseriate NGT were observed in the species *C. uniflora*, *S. chilensis* and *S. trilobata* (Figs. 7A, G–H and 8A, G–H″). *C. nutans* presented long and numerous trichomes (Figs. 7B and 8B). The *Lychnophora* species

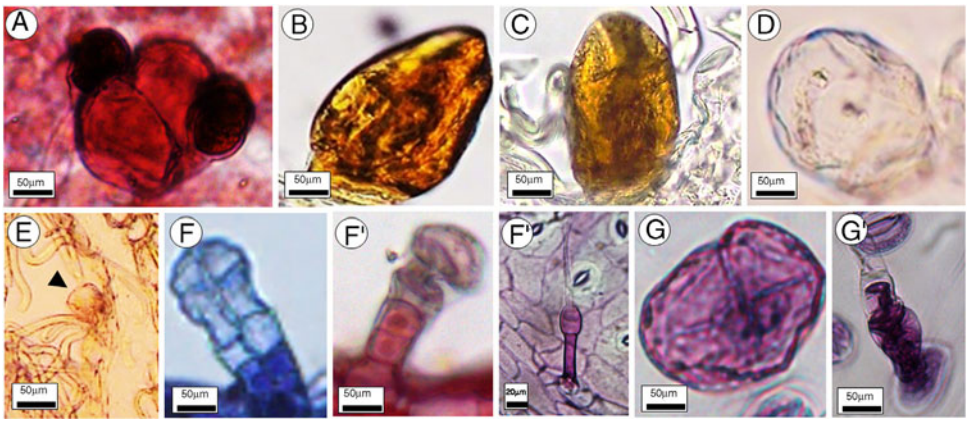

Fig. 5. Glandular trichome (GT) in cross-sections of leaves fully expanded of "arnicas". Light microscopy: A. *Calea uniflora*; B. *Lychnophora diamantinana*; C. *Lychnophora ericoides*; D. *Lychnophora pinaster*; E. *Lychnophora salicifolia;* F, F′, F″. *Solidago chilensis*; G, G′. *Sphagneticola trilobata*; A, F′, F″, G and G′. staining with safranine; F. staining with toluidine blue; B, C, D, E. uncolored. Findings: A. GT inserted in small depression and multicellular and bicellular or capited with unicellular pedicel and globoid head. B–D. GT inclosed in crypts; F. GT multicellular plurisseriate and/or capitate with unicellular pedicel with elongated terminal cell; G. GT bisseried in depression and/or multicellular unisseriate with elongated terminal cell.

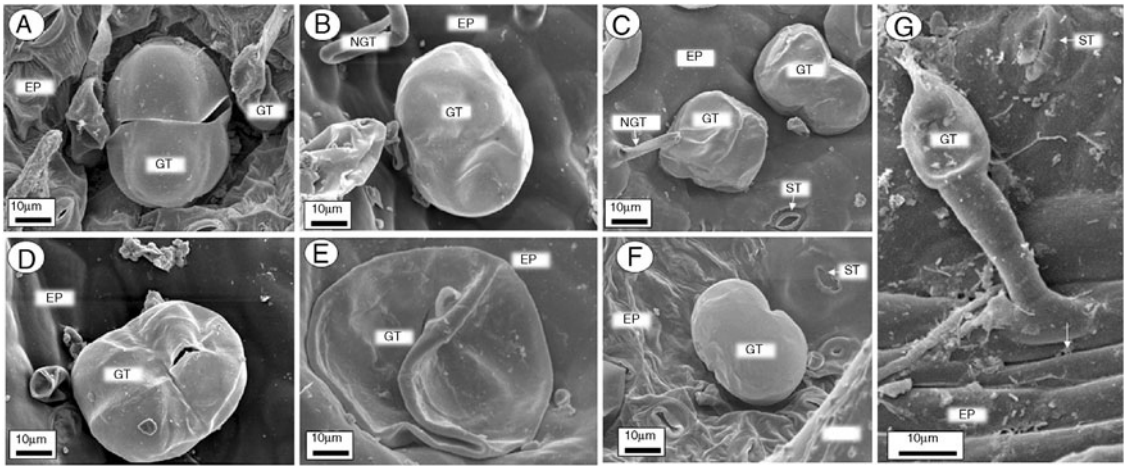

Fig. 6. Glandular trichome (GT) of leaves fully expanded of "arnicas" by SEM. A. *Calea uniflora*; B. *Lychnophora diamantinana*; C. *Lychnophora ericoides*; D. *Lychnophora pinaster*; E. *Lychnophora salicifolia*; F. *Sphagneticola trilobata*; G. *Solidago chilensis*. Abbreviations: EP, epidermis; ST, stoma; GT, glandular trichome; NGT, non glandular trichome. Findings: A. GT inserted in small depression and multicellular and bicellular or capited with unicellular pedicel and globoid head; B–D. GT inclosed in crypts; F. GT multicellular plurisseriate and/or capitate with unicellular pedicel with elongated terminal cell; G. GT bisseried in depression and/or multicellular unisseriate with elongated terminal cell.

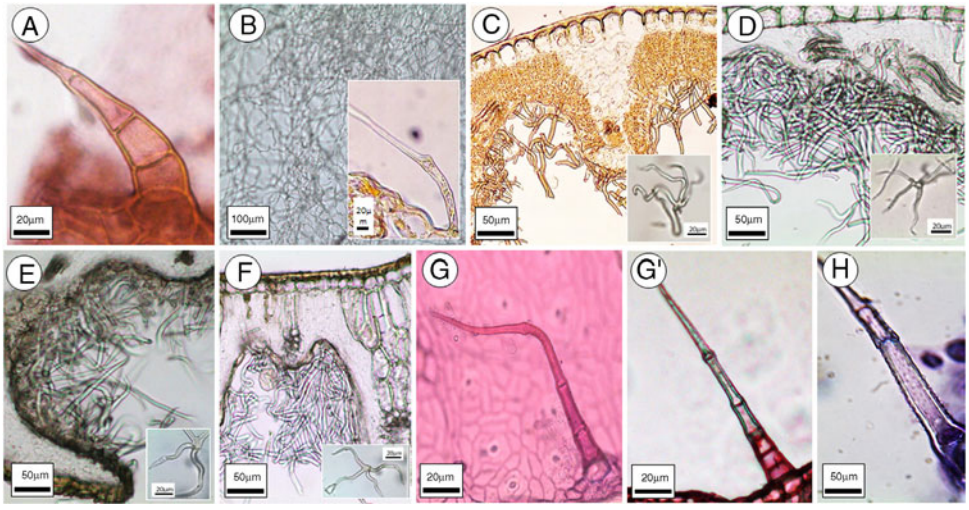

Fig. 7. Non glandular trichome (NGT) in cross section of leaves fully expanded of "arnicas". A. *Calea uniflora*; B, B′. *Chaptalia nutans*; C. *Lychnophora diamantinana*; D. *Lychnophora ericoides*; E. *Lychnophora pinaster*; F. *Lychnophora salicifolia*; G, G′. *Solidago chilensis*; H. *Sphagneticola trilobata*; Findings: A, G, G′, H. staining with safranine; B, C, D, E, F. uncolored; A, G, G′, H. multicellular (5–8 cells) and unisseriate NGT; B. long and numerous NGT; C, F. starred trichomes (3–5 arms); G, G′. elongated TNG, with slightly enlarged base and slim terminal cell; H. NGT with the basal cell of verrucous cuticle.

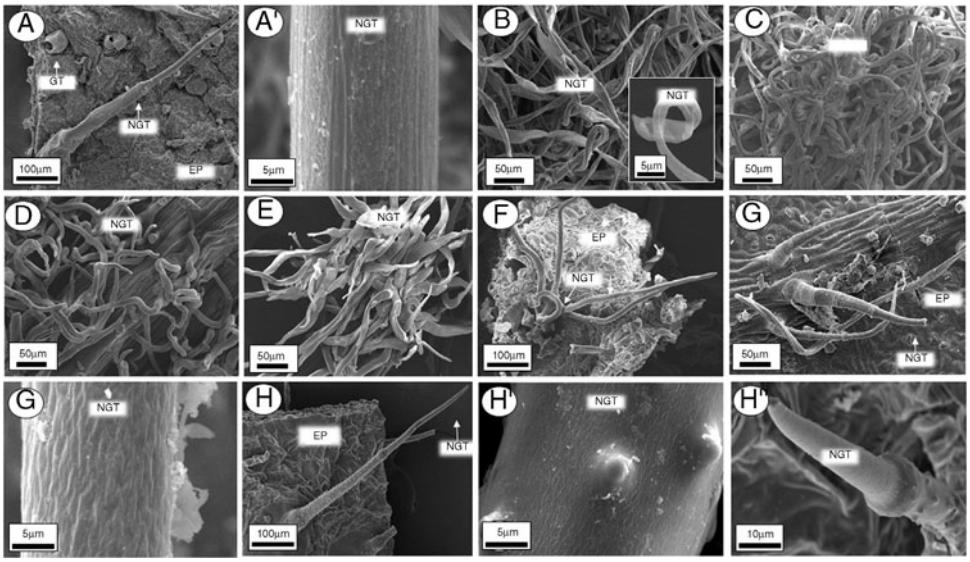

Fig. 8. Non-glandular trichome (NGT) of leaves fully expanded of "arnicas" by SEM. A, A′. *Calea uniflora*; B, B′. *Chaptalia nutans*; C, C′. *Lychnophora diamantinana*; D. *Lychnophora ericoides*; E. *Lychnophora pinaster*; F. *Lychnophora salicifolia*; G. *Solidago chilensis*; H, H′, H″. *Sphagneticola trilobata*; Abbreviations: EP, epidermis; ST, stoma; GT, glandular trichome; NGT, non glandular trichome. Findings: A, G–H. multicellular (5–8 cells) and unisseriate NGT; B. long and numerous NGT; C–F. starred trichomes (3–5 arms); G. elongated TNG, with slightly enlarged base and slim terminal cell; H. NGT with the basal cell of verrucous cuticle.

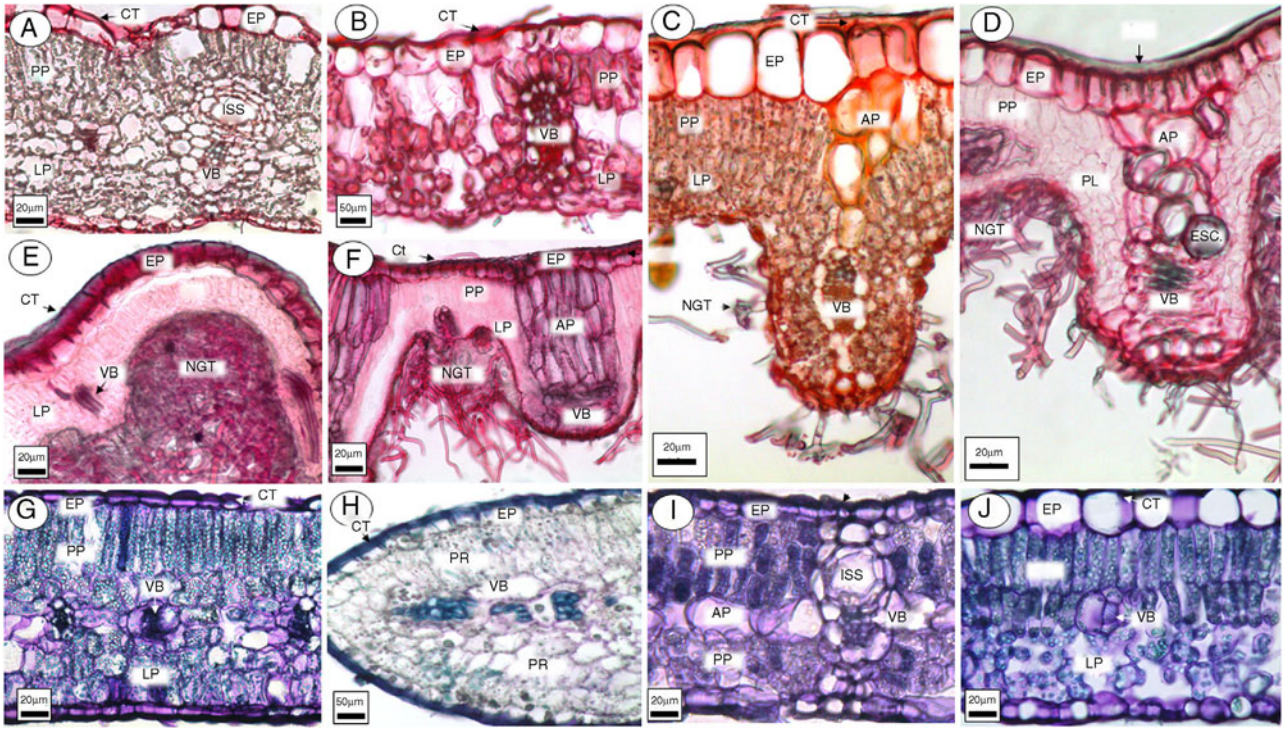

Fig. 9. Intermediate region of mesophyll (IRM) in cross section of leaves fully expanded of "arnicas". A. *Calea uniflora*; B. *Chaptalia nutans*; C. *Lychnophora diamantinana*. D. *Lychnophora ericoides*; E. *Lychnophora pinaster*; F. *Lychnophora salicifolia*; G. *Porophyllum ruderale*; H. *Pseudobrickellia brasiliensis*; I. *Solidago chilensis*; J. *Sphagneticola trilobata.* Abbreviations: CUT, cuticule; PP, palisade parenchyma; LP, lacunar parenchyma; AP, aquiferous parenchyma; PR, regular parenchyma; VB, vascular bundle blond; ESC, sclerehyde; EP, epidermis; GT, glandular trichome; NGT, non-glandular trichome; IC, internal cavity. Findings: A–F. staining with ruthenium red; G, J. staining with toluidine blue; A, B, G, J. dorsiventral parenchyma; C–F. palisade (adaxial), spongy (abaxial) and aquiferous parenchyma strata close to the vascular bundles with extension of the bundle sheath; H. homogenous mesophyll; I. isobilateral mesophyll and aquiferous parenchyma (interconnecting the vascular bundles); A–J. collateral type of the bundles.

presented starred trichomes (3–5 arms) varying in size and width, with cellulosic thickening and concentrated on the abaxial face of the leaf between crypts (Figs. 7C–F and 8C–F). *S. chilensis* showed elongated TNG, with slightly enlarged base and slim terminal cell (Figs. 7G–G′ and 8G–G′′). *S. trilobata* presented trichomes with the basal cell of verrucous cuticle (Figs. 7H and 8H–H′′).

The intermediate region of the mesophyll (IR) was dorsiventral parenchyma for the species *C. uniflora*, *C. nutans*, *P. ruderale* and *S. trilobata* (A, B, G, J). The *Lychnophora* species presented palisade (adaxial), spongy (abaxial) and aquifer parenchyma strata close to the vascular bundles with extension of the bundle sheath, except to *L. pinaster* (Fig. 9C–F). *P. brasiliensis* presented

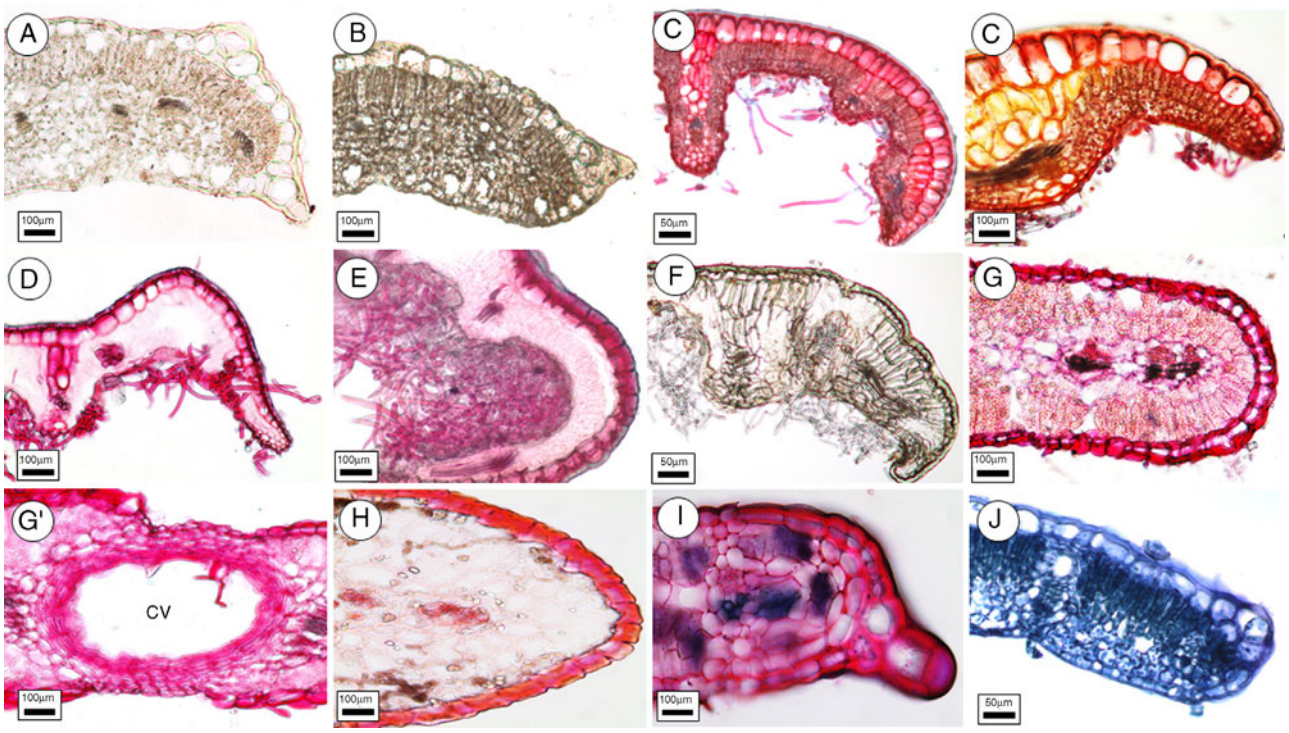

Fig. 10. Leaf margin in cross section of leaves fully expanded of "arnicas". A. *Calea uniflora*; B. *Chaptalia nutans*; C, C′. *Lychnophora diamantinana*; D. *Lychnophora ericoides*; E. *Lychnophora pinaster*; F. *Lychnophora salicifolia*; G, G′. *Porophyllum ruderale*; H. *Pseudobrickellia brasiliensis*; I. *Solidago chilensis*; J. *Sphagneticola trilobata*; A, B, F. staining with ferric chloride; C–E and G–I. staining with ruthenium red; J. toluidine blue. Findings: A–F, J. rounded and flexed sheet edge for the abaxial face; C–F. flexion with a final margin narrowing. I. discrete flexion of the margin with epidermal projections to the outside of the leaf; G–H. straight margin, without flexion or little flexure. G, G′. large secretory cavity on the margin of leaf.

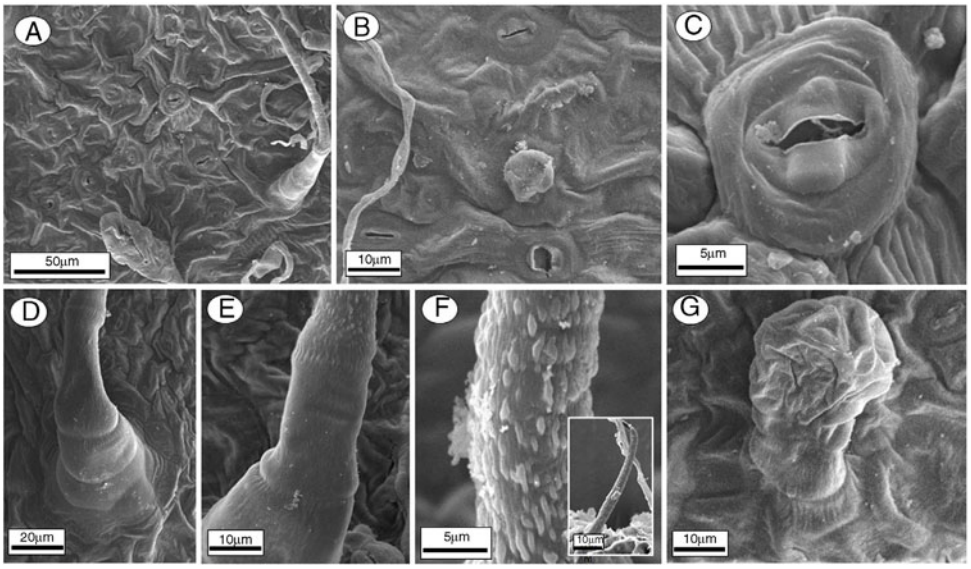

Fig. 11. Analyses of leaves fully expanded of *Arnica montana* by SEM. A. adaxial face; B. abaxial surface; C. stomata; D. base of the NGT; E. peduncle of NGT; F. apex of NGT. G. GT.

homogenous mesophyll, without distinction between the cells (Fig. 9H). *S. chilensis* presented mesophyll of the isobilateral type with presence of aquifer parenchyma in the medial region of the mesophyll and interconnecting the vascular bundles (Fig. 9I). In all species, the bundles were of the collateral type, distributed in the median region of the mesophyll, being surrounded by a parenchymatic sheath. In the species *C. uniflora* and *S. chilensis*, these may be associated with secretory ducts (Fig. 9A, I). The *Lychnophora* presented extension of the sheath of the bundle and also larger dimensions of the region where the vascular bundles meet (Fig. 9C–F). The presence of crystal idioblasts was verified in the *L. diamantinana* (small druses). The occurrence of phenolic, lipophilic and pectic compounds was also verified (Item 4.2).

Leaf margin

In the present study, among the "arnica" specimens, there was a difference in leaf margin in relation to flexion and distribution of parenchyma cells. The species *C. uniflora*, *C. nutans*, *L.*

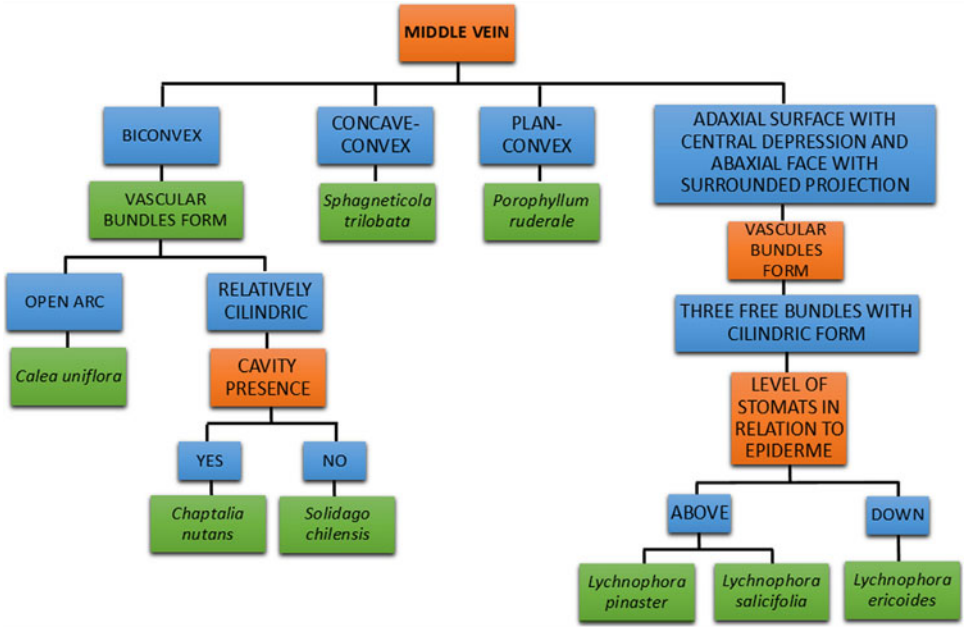

Fig. 12. Flowchart to quality control of the "arnicas" evaluated using the leaves fully expanded, through the middle vein. Orange, anatomical parameters; Blue, anatomical definition and target; Green, specie confirmation.

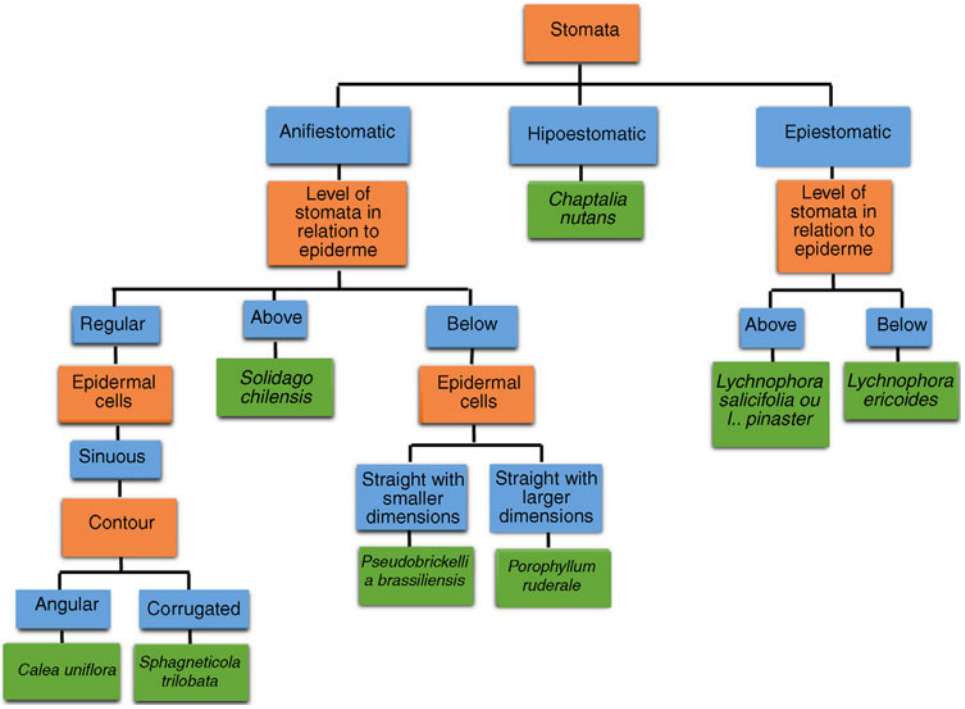

Fig. 13. Flowchart to quality control of the "arnicas" evaluated using the leaves fully expanded, through the stomata. Orange, anatomical parameters; Blue, anatomical definition and target; Green, specie confirmation.

ericoides, *L. diamantinana*, *L. pinaster*, *L. salicifolia* and *S. trilobata* showed rounded and revolute leaf border toward the abaxial face (Fig. 10A–F, J). For the *Lychnophora* species there is marked flexion with a final margin narrowing (Fig. 10C–F). *S. chilensis* presented discrete flexion of the margin and with epidermal projections to the outside of the leaf (Fig. 10I). On the other side, the species *P. ruderale* and *P. brasiliensis* showed a straight margin, without or little flexion (Fig. 10G–H). In particular, there is a large secretory cavity present on the margin of *P. ruderale* (Fig. 10G–G′). The organization of the mesophyll cells follows the same distribution of the intermediate portion, with exception for *S. chilensis* with predominance of aquifer parenchyma (Fig. 10I).

A. montana *("the true* Arnica*")*

Analyses of the *A. montana* leaves were performed only by scanning electron microscopy (Fig. 11A–G). We are observed the amphistomatic pattern of the leaves, with a greater number of stomata on the abaxial face of the leaf (Fig. 11A and B). Stoma was lightly projected onto the epidermis (Fig. 11C). The non-glandular trichomes (4–5 cells) showed a verrucous apical cell and smooth

Fig. 14. Flowchart to quality control of the "arnicas" evaluated using the leaves fully expanded, through the trichomes. Orange, anatomical parameters; Blue, anatomical definition and target; Green, specie confirmation.

cuticle to the base cells (Fig. 11A–B, D–F). The glandular trichomes are capitate (Fig. 1G).

Identification flowchart for the "arnicas" evaluated in this study

To systematize the micromorphological characterization of the "arnicas" evaluated in this study, a flowchart was created to differentiate the species. Diagnostic anatomical elements were identified and plotted making possible the quick identification of species, intact or crushed (Figs. 12–14).

Histochemical characterization

The histochemical tests revealed that secondary metabolites the main chemotaxonomic markers of the "Arnicas" were secreted and accumulated in specifics secretory structures such as glandular trichomes, epidermal idioblasts, secretory tissues such as palisade and spongy chlorophyll parenchyma, the middle vein in the leaves and in the internal secretory structures. The figures show positive reactions to: lipophilic substances, evidenced by Sudan IV (Figs. 15 and 16) in orange to red; sesquiterpene lactones evidenced by sulphuric acid (Figs. 17 and 18) in red to orange and yellow and phenolic compounds evidenced by ferric chloride (Figs. 19 and 20) with brown color.

The histochemical reactions, classes of metabolites found and the sites of secretion in the evaluated species will be show in Table 2.

Chemical review

The phytochemical review of the species of "arnica" reveals diversification of compounds. Based on the data obtained, is possible verify the main classes of metabolites in each of the species (Fig. 21). Table 3 compiles the literary findings referring to the main substances described for each of the species.

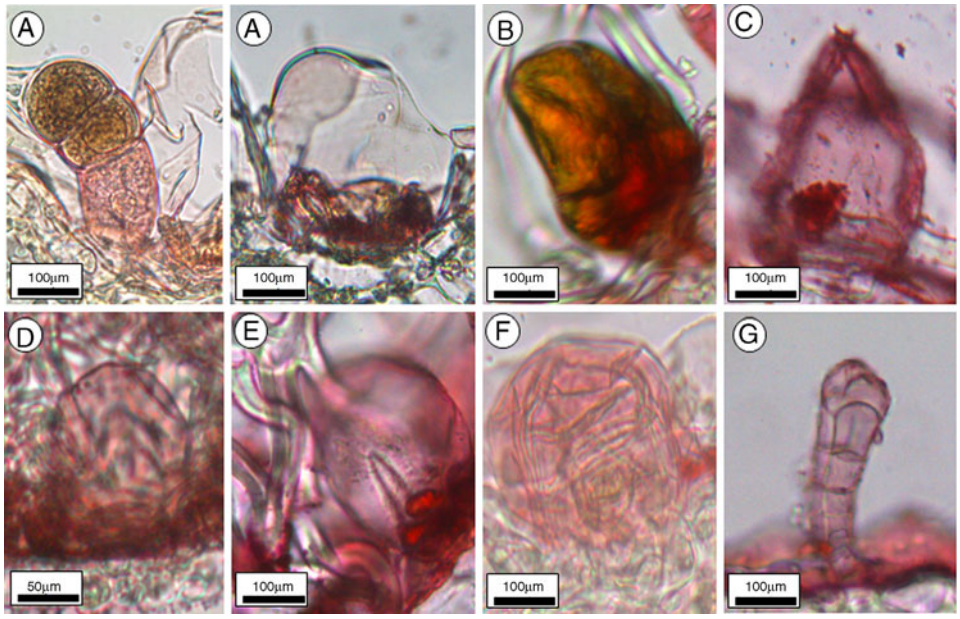

Fig. 15. Histochemical reaction for lipophilic substances in cross-sections of leaves of "arnicas", highlighted by Sudan. Light microscopy. The figure shows positive reactions (red) for lipophilic substances with accumulation of metabolites in glandular trichomes. A, A′. *Calea uniflora*; B, B′. *Lychnophora diamantinana*; C. *Lychnophora ericoides*; D. *Lychnophora pinaster*; E. *Lychnophora salicifolia*; F. *Solidago chilensis*; G. *Sphagneticola trilobata*.

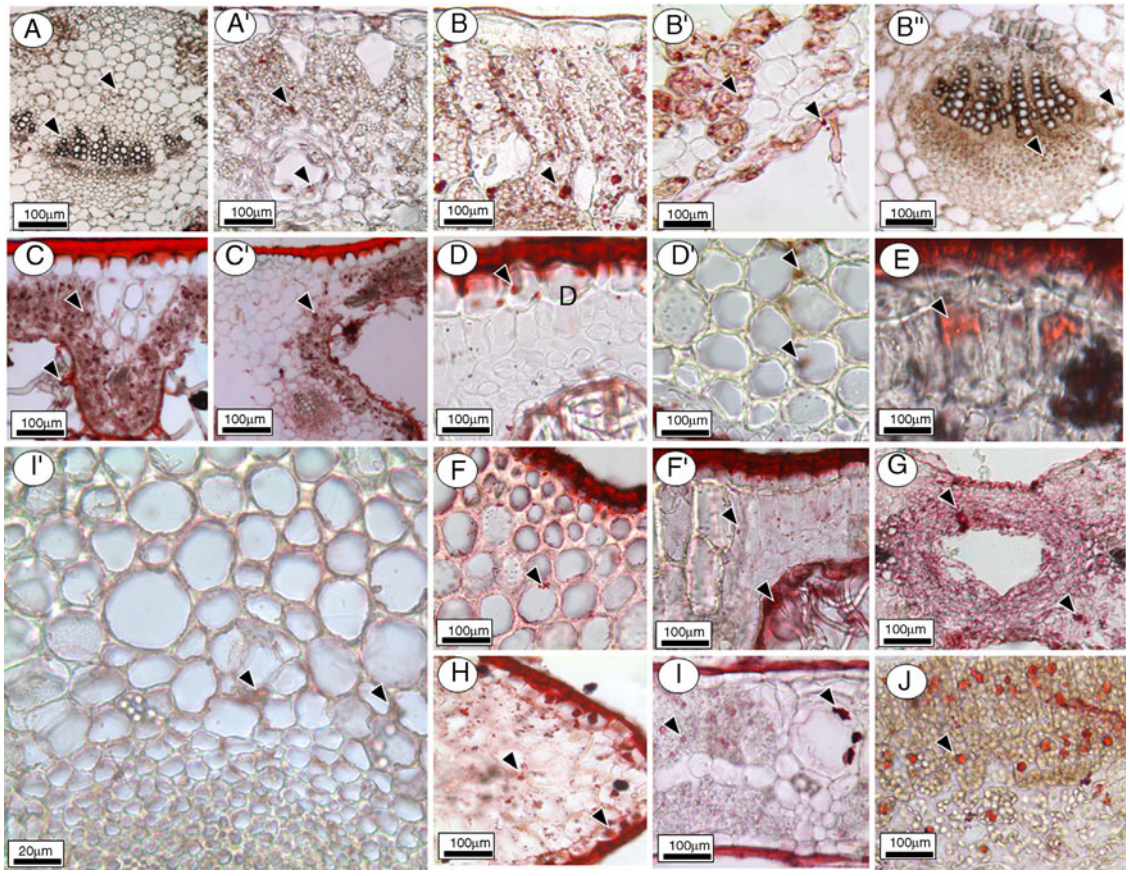

Fig. 16. Histochemical reaction for lipophilic substances in cross-sections of leaves of "arnicas", highlighted by Sudan. Light microscopy. The figure shows positive reactions for lipophilic substances with accumulation and secretion of metabolites in the epidermal cells and other secretory structures of leaves. A, A′. *Calea uniflora*; B. *Lychnophora diamantinana*; C. *Lychnophora ericoides*; D. *Lychnophora pinaster*; E. *Lychnophora salicifolia*; F. *Solidago chilensis*; G. *Sphagneticola trilobata*. Findings: A, B″, C′, D′, I′, F′. midvein with accumulation of metabolites in parenchyma cells. A′, B, B′, C, D, D′, E, F′, G, H, I, J. accumulation of metabolites in the epidermis and/or chlorophyll parenchyma of the mesophyll; A, A′, G, I, I′. accumulation of metabolites in the internal secretory structure. Reaction pattern at the tip of the arrow (red).

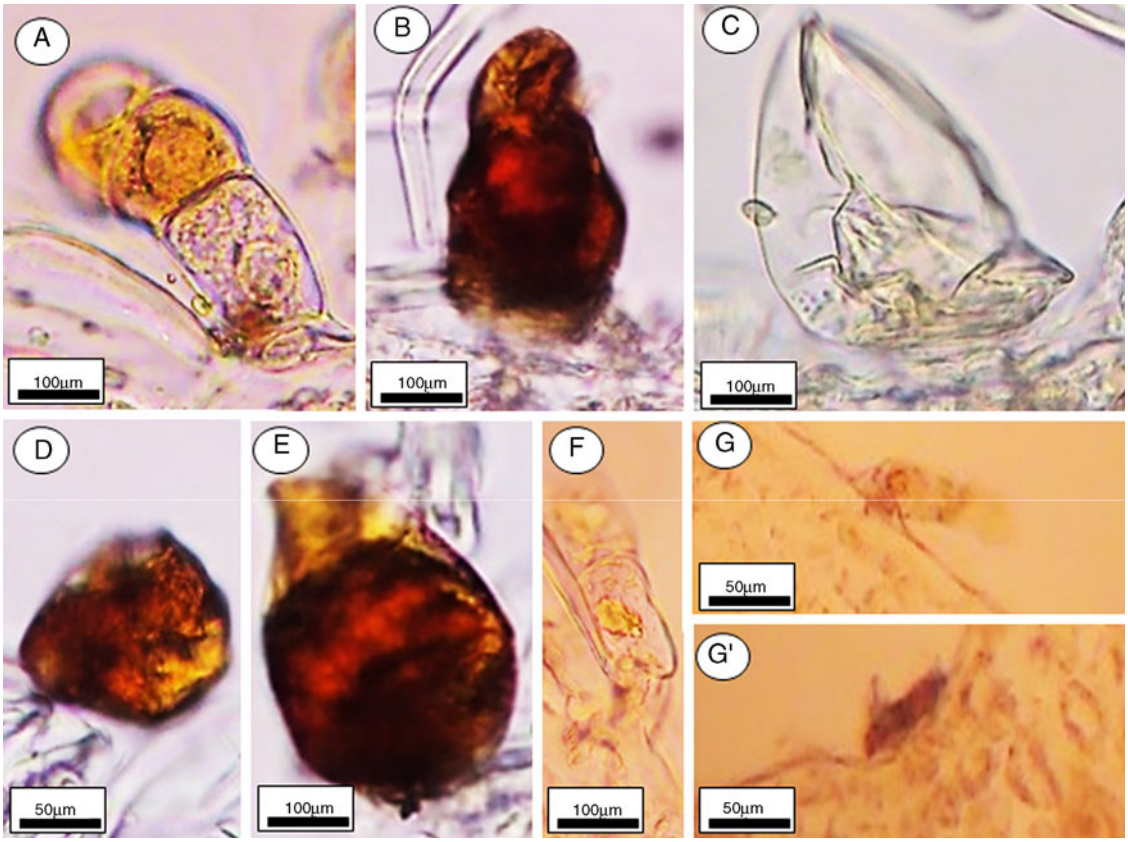

Fig. 17. Histochemical reaction for screening of sesquiterpene lactones in cross-sections of leaves of "Arnicas", evidenced by sulphuric acid. Light microscopy. The figure shows positive reactions (brown/orange) for screening of sesquiterpene lactones with accumulation of metabolites in glandular trichomes. A. *Calea uniflora*; B. *Lychnophora diamantinana*; C. *Lychnophora ericoides*; D. *Lychnophora pinaster*; E. *Lychnophora salicifolia*; F. *Solidago chilensis*; G, G′. *Sphagneticola trilobata*.

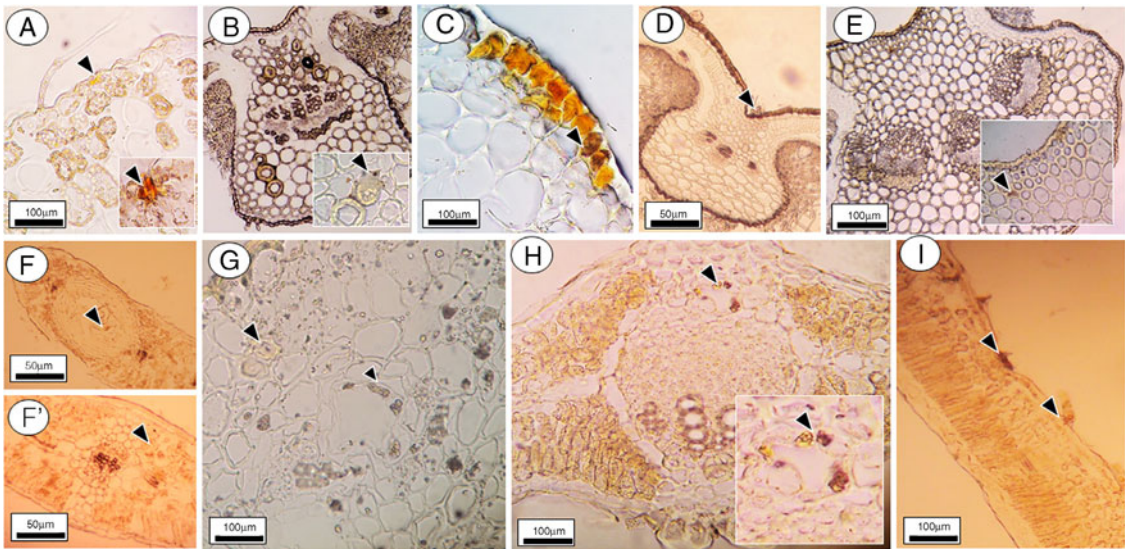

Fig. 18. Histochemical reaction for screening of sesquiterpene lactones in cross-sections of leaves of "arnicas", evidenced by sulphuric acid. Light microscopy. The figure shows positive reactions for screening of sesquiterpene lactones with accumulation and secretion of metabolites in the epidermal cells and other secretory structures of leaves. A. *Calea uniflora*; B. *Lychnophora diamantinana*; C. *Lychnophora ericoides*; D. *Lychnophora pinaster*; E. *Lychnophora salicifolia*; F. *Solidago chilensis*; G. *Sphagneticola trilobata*. Findings: B, D, E, F′, H. midvein with accumulation of metabolites in parenchyma cells; A, C, F, G, H, I. accumulation of metabolites in the epidermis and/or chlorophyll parenchyma of the mesophyll; F, G, H. accumulation of metabolites in the internal secretory structure. Reaction pattern at the tip of the arrow (brown/orange).

Discussion

Micromorphological characterization

The anatomical data observed in the middle vein (MV) for the species *C. uniflora*, *C. nutans* and *S. chilensis* are in agreement with those described by Budel et al. (2006), Empinotti and Duarte (2006) and Souza et al. (2017), respectively. The MV observed in *S. trilobata* and *P. ruderale* was according to Baccarin et al. (2009) and Milan et al. (2006), respectively. The leaves of the *Lychnophora* are relatively similar: the MV of *L. salicifolia*, *L. pinaster* and *L. diamantinana* presented adaxial face with central depression and abaxial

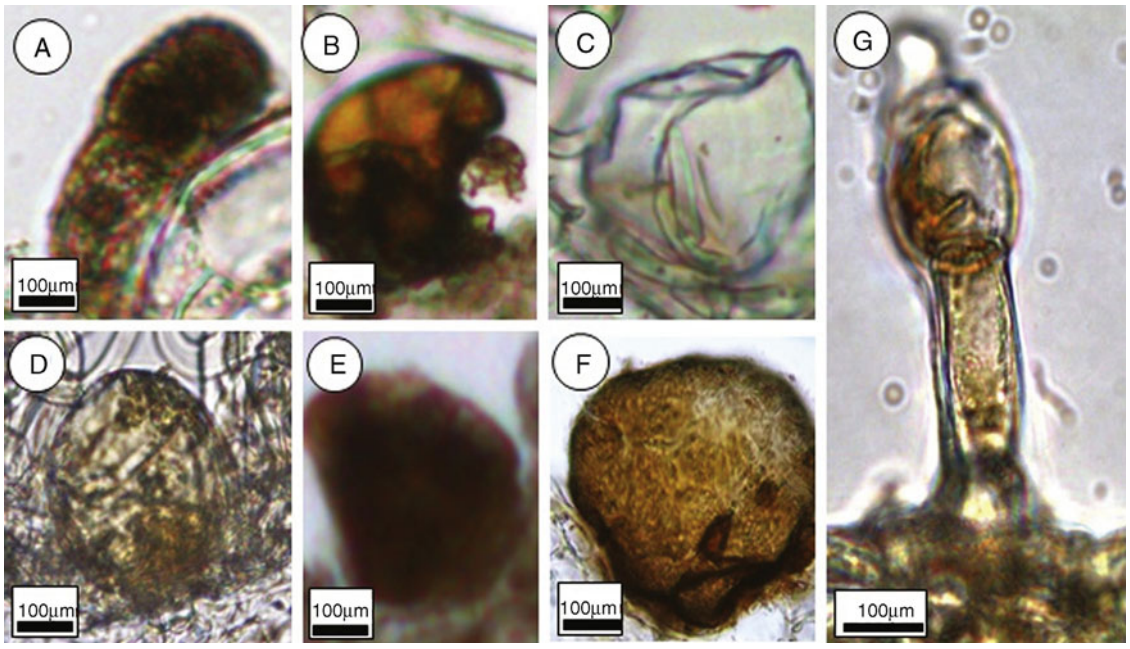

Fig. 19. Histochemical reaction for phenolic substances in cross-sections of leaves of "arnicas", highlighted by ferric chloride. Light microscopy. The figure shows positive reactions (brown) for phenolic substances with accumulation of metabolites in glandular trichomes. A. *Calea uniflora*; B. *Lychnophora diamantinana*; C. *Lychnophora ericoides*; D. *Lychnophora pinaster*; E. *Lychnophora salicifolia*; F. *Solidago chilensis*; G. *Sphagneticola trilobata*.

Table 2
Histochemical tests and suggested metabolic classes for leaf secretions of "Arnicas" species.

Species	Histochemical tests Metabolic classes	Sudan IV Lipophilic substances	Sulphuric acid Sesquiterpene lactones	Ruthenium red Pectic compounds	Ferric chloride Phenolic compounds
Arnica montana		*IR, GT, MD SS*	*Not identified*	*IR, GT, MD, EP*	*IR, MS, MD*
Calea uniflora		*IR, GT, MD SS*	*IR, GT*	*GT, SS*	*IR, GT, MD, SS*
Chaptalia nutans		*IR EP*	*IR, MD,*	*IR, SS*	*MS*
Sphagneticola trilobata		*IR, GT, MD, SS EP*	*IR, GT*	*IR, GT, MD, SS*	*IR, GT, MD, SS*
Solidago chilensis		*IR, GT SS*	*IR, GT, MD, SS*	*IR, GT, SS, NGT*	*IR, GT, MD, SS*
Porophyllum ruderale		*IR, MD, SS*	–	*IR, MD, SS*	*IR, MD, SS*
Pseudobrickellia brasiliensis		*MS*	*SS, MS*	*MS*	*MS*
Lychnophora ericoides		*IR, GT, MD*	*GT, MD*	*IR, MD, NGT*	*IR, GT, MD, NGT*
Lychnphora saicifolia		*IR, GT, MD*	*GT*	*IR, GT, MD, NGT*	*IR, GT, MD, NGT*
Lychnophora pinaster		*IR, GT, MD*	*GT*	*IR, MD, NGT*	*IR, GT, MD, NGT*
Lychnophora diamantinana		*IR, GT, MD, NGT*	*GT, MD*	*IR, GT, MD, NGT, EP*	*IR, GT, MD, NGT*

IR, intermediate mesophyll region; EP, epidermal cells; ST, stomata; MV, middle vein; GT, glandular trichome; NGT, non-glandular trichome; MS, mesophyll; "–", negative; SS, secretory structure.

surface with rounded projection. *L. ericoides* presented on the adaxial face discrete central depression and abaxial surface also with rounded projection. Through the characterization of the MV of the "arnica" species, it was possible to obtain a preliminary differentiation among the evaluated species, especially in relation to the form of MV, being an important anatomical character for quality control.

In relation to epidermal attachments, we observe variable structures of great diagnostic value for taxonomy, such as glandular trichomes (GT) that are involved in the secretion of various bioactive substances (Lusa et al., 2016a,b). In the present study, different types of GT were described, being able to be used for quality control of the species. The findings regarding *S. chilensis* differ from those registered by Souza et al. (2017) that describes, through paradermal sections, only the presence of non-glandular trichomes in the leaves of the specie, while we observed the presence of non-glandular trichomes and glandular trichomes in cross-sections. In *S. trilobata* the GT were present in two forms: bisseriate in depression and a multicellular with elongated apex, identified for the first time. For *C. uniflora*, the GT are according to description made by Budel et al. (2006). For the *Lychnophora* genus, GT were detected on the abaxial surface, between the crypts. These data are correlate with those described by Lusa et al. (2016a,b) for other *Lychnophora* species. No glandular trichomes was found in the species *P. ruderale* and *C. nutans*, in agreement with described by Empinotti and Duarte (2006) and Duarte et al. (2007), respectively. In *P. brasiliensis* no GT was observed either.

Some anatomical diagnostic features were observed through non glandular trichomes (NGT). In *P. ruderale*, a leaf glabrous was observed, without the trichomes previously described by Duarte et al. (2007). The absence of hairs was also observed for *P. brasiliensis*. In *C. nutans* numerous NGT were found predominantly on the abaxial surface (Empinotti and Duarte, 2006). In relation to *S. chilensis*, *S. trilobata* and *C. uniflora*, similar anatomical findings were described by Souza et al. (2017), Baccarin et al. (2009) and Budel et al. (2006).

According to Metcalfe and Chalk (1988) anomocytic stomata are characteristic of the Asteraceae family, as we observed predominantly. For the *Lychnophora* it was not possible to characterize the type of stomata due to the innumerable presence of non-glandular trichomes and also by the stomata being inserted in the crypts, making their visualization even more difficult.

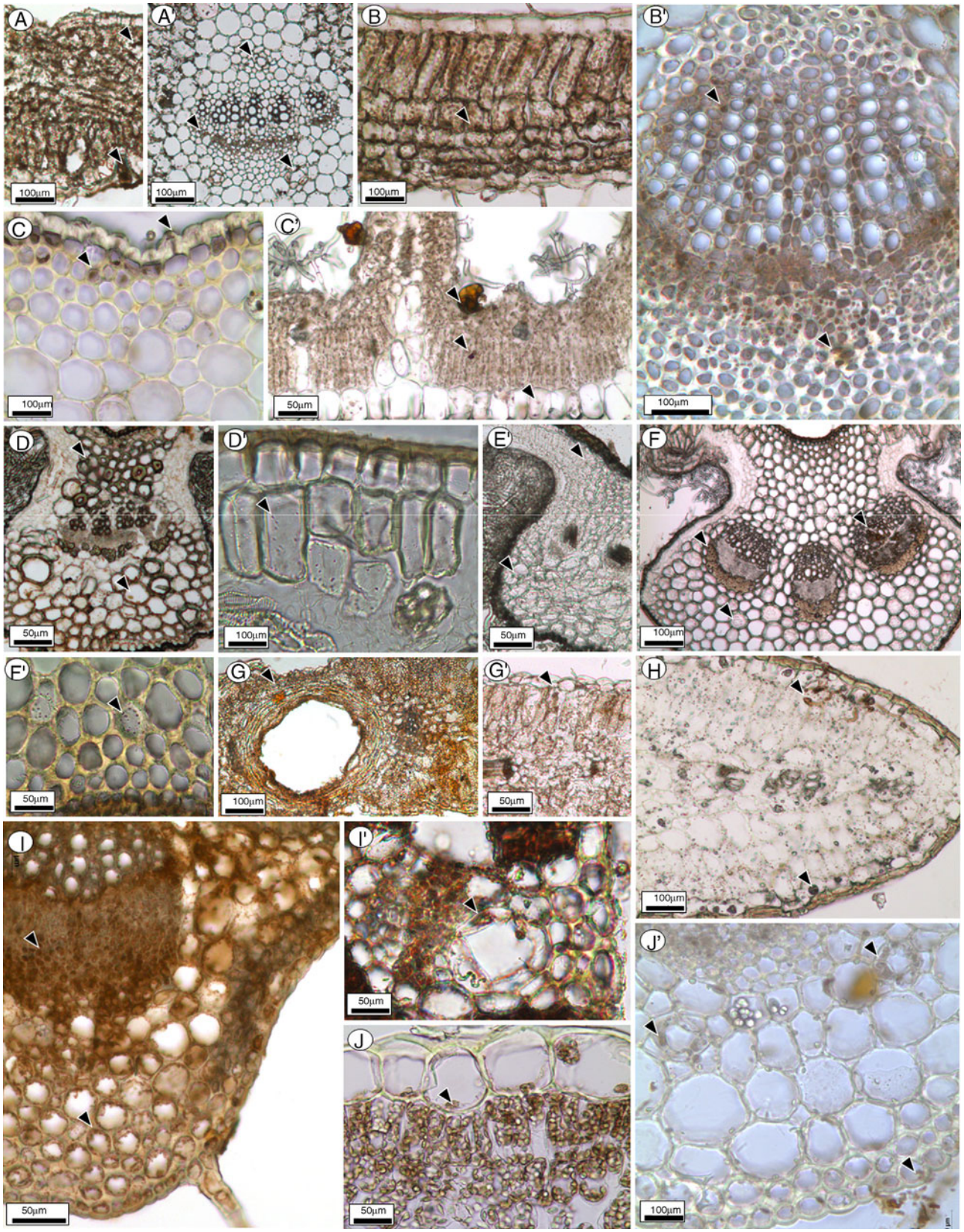

Fig. 20. Histochemical reaction for phenolic substances in cross-sections of leaves of "arnicas", highlighted by ferric chloride. Light microscopy. The figure shows positive reactions for phenolic substances with accumulation and secretion of metabolites in the epidermal cells and other secretory structures of leaves. A. *Calea uniflora*; B. *Lychnophora diamantinana*; C. *Lychnophora ericoides*; D. *Lychnophora pinaster*; E. *Lychnophora salicifolia*; F. *Solidago chilensis*; G. *Sphagneticola trilobata*. Findings: A′, B′, C, D, E, F, F′, I, J′. midvein with accumulation of metabolites in parenchyma cells; A, B, C, D′, G, G′, H, I, J. accumulation of metabolites in the epidermis and/or chlorophyll parenchyma of the mesophyll; A′, G, I′, J. accumulation of metabolites in the internal secretory structure. Reaction pattern at the tip of the arrow (brown).

Table 3
Review of main compounds described for the known species of the "arnicas" in Brazil.

Compounds	*A. montana*	*S. trilobata*	*S. chilensis*	*C. uniflora*	*P. ruderale*	*C. nutans*	*P. brasiliensis*	*L. ericoides*	*L. salicifolia*	*L. pinaster*	*L. diamantinana*
Flavone											
Apigenin								x[F,G]			
Apigenin glycosylated								x[F,G]			
Chrysin								x[F]	x[K]	x[K]	x[G]
Chrysin glycosyl								x[F,G]			
Luteolin		x[k]	x[a]				x[C]				
Luteolin glycosil								x[F]			
3′,4′,7-Trihydroxi-flavone-7-*O*-β-glucopyranosyl				x[s]							
5,4′-Dihydroxy-7-methoxyflavone		x[j]									
5,3′,4′-Trihydroxy-7-methoxyflavone		x[j]									
5,7-Dihydroxy-4′-methoxyflavone (acacetin)								x[F]			
3,7,4′-Trihydroxyflavanone (garbanzol)								x[F]			
3-Methyl-galangin								x[F]			
Flavanone											
Naringenin								x[F,G]			
Pinocembrin								x[F,G]	x[K]	x[K]	x[G]
Pinostrobin								x[F,G]	x[K]	x[K]	x[G]
Naringenin								x[F,G]			
Pinocembrin								x[F,G]	x[K]	x[K]	x[G]
Pinobanksin								x[F,G]	x[K]		x
Flavonol											
Afzelechin			x[a]								
Galangin								x[F]			
Kaempferol	x[N]		x[a]								
Resokaempferol								x[F]			
Patuletin	x[N]		x[a]								
Quercetin	x[N]	x[k]	x[b]	x[s]	x[v]	x[A]	x[C]	x[F,G]	x[J]	x[M]	
Quercetin heterozyl	x[N]	x[k]	x[a]	x[s]							
Quercetin-7,3′,4′-trimethyl ether									x[J]		
Quercetol								x[F,G]			
Rutin	x[N]				x[v]						
Chalcone											
Butein chalcona				x[r]							
Butein 4′-*O*-glucopyranosyl				x[r]							
α-Hydroxy-butein				x[r]							
2′,4-Hihydroxy-3-methoxy-chalcone-4′-*O*-β-glucopyranosyl				x[s]							
2′,4′,3,4-α-Pentahydroxychalcone				x[s]							
Pinostrobin chalcone								x[F,G]			

Table 3 (*Continued*)

Compounds	*A. montana*	*S. trilobata*	*S. chilensis*	*C. uniflora*	*P. ruderale*	*C. nutans*	*P. brasiliensis*	*L. ericoides*	*L. salicifolia*	*L. pinaster*	*L. diamantinana*
Coumarins											
Umbeliferone	x(O)										
Escopoletin	x(O)					x(B)					
7-*O*-β-D-Glucopyranosyl-nutanocoumarin						x(B)					
4-*O*-fl-Gluco-pyranosyl-5-methylcoumarin						x(B)					
9′-*O*-fl-D-Glucopyranosyl-nutanocoumarin						x(B)					
Nutanocumarin						x(B)					
Chromene											
Eugenin				x(r)							
Noreugenin				x(r)							
Chromanone											
2,2-Dimethyl-6-(1-hydroxy-ethyl)-chromanone				x(t)							
Uniflorol b				x(t)							
Uniflorol a				x(t)							
Organic acid derivatives											
Quinic acid	x(O)		x(c,d)	x(u,r)	x(v)						
Caffeic acid	x(O)		x(c)	x(u,r)						x(L)	
Gallic acid			x(d)	x(r)	x(v)						
Ethyl caffeate		x(m)		x(r)							
Cinnamic acid										x(L)	
3-*O*-Caffeoylquinic acid	x(O)	x(l)	x(c)	x(r)					x(J)		
4-*O*-Caffeoylquinic acid								x(F)	x(J)		
5-*O*-Caffeoylquinic acid									x(J)	x(L)	
3,4-*O*-Caffeoylquinic acid		x(l)	x(c)	x(r)					x(J)		
4,5-*O*-Caffeoylquinic acid		x(l)	x(c)	x(r)				x(F)	x(J)		
3-*O*-*p*-Coumaroylquinic acid									x(J)		
4-*O*-*p*-Coumaroylquinic acid									x(J)		
5-*O*-*p*-Coumaroylquinic acid									x(J)		
3-*O*-*E*-Coumaroyl,5-*O*-*p*-caffeoylquinic acid									x(J)		
3-*O*-*E*-Caffeoyl,5-*O*-*p*-coumaroylquinic acid									x(J)		
4-*O*-Feruloyl 5-*O*-caffeoylquinic acid									x(J)		
3,4-di-*O*-*p*-Coumaroylquinic acid									x(J)		
4-Caffeoyl-5-feruloylquinic acid								x(F)			
4,5-Diferuloylquinic acid								x(F)			
3-*O*-Feruloylquinic acid								x(F)			
4-*O*-Feruloylquinic acid								x(F)			
5-*O*-Feruloylquinic acid								x(F)	x(J)		
4-Hydroxy-3-methoxybenzoic acid (vanillic acid)		x(j)		x(s)							
2-Senecioyl-4-(methoxy-ethyl)-phenol				x(s)							

Table 3 (*Continued*)

Compounds	*A. montana*	*S. trilobata*	*S. chilensis*	*C. uniflora*	*P. ruderale*	*C. nutans*	*P. brasiliensis*	*L. ericoides*	*L. salicifolia*	*L. pinaster*	*L. diamantinana*
2-Senecioyl-4-(angeloyloxy-ethyl)-phenol				x(s)							
2-Senecioyl-4-(pentadecanoyloxy-ethyl)-phenol				x(s)							
2-Senecioyl-4-(hydroxy-ethyl)-phenol				x(s)							
Protocatechuic acid									x(J)		
Monoterpenes											
α-Pinene		x(n)	x(f)		x(x)		x(D)				
β-Pinene		x(n)	x(f)		x(x)		x(D)				
Mircene		x(n)	x(f)		x(x)						
δ-3-Carene			x(f)								
β-Ocimene		x(n)	x(f)		x(x)						
Sesamol			x(f)								
Isolongifolene			x(f)								
Biciclogermacrene			x(f)								
1,10-di-*epi*-Cubenol			x(f)								
α-Cadinol			x(f)								
Cubenol			x(f)								
Sabinene		x(n)	x(f)								
Terpin-4-ol			x(f)		x(x)		x(D)				
p-Cimen-8-ol			x(f)								
β-Bourbonene			x(f)								
γ-Gurjunene			x(f)								
α-Thujene		x(n)									
1,3,8-*p*-Menthatriene		x(n)									
α-Campholenal		x(n)									
Tetrachyrin		x(n)									
β-Cubebene					x(x)						
Elemene					x(x)						
Isocomene					x(x)						
Sabinene					x(x)						
2,3-Dihidro-1,8-cineole					x(x)						
Terpinolene					x(x)						
trans-β-Ocimene					x(x)						
β-Ciclocitral					x(x)						
Cuminol					x(x)						
α-Terpinene							x(D)				
γ-Terpinene							x(D)				
α-Terpineol							x(D)				
(−)-Germacra-1(10),5(e)-dien-4β-ol							x(D)				
Cumene	x(R)										
Camphene	x(R)	x(n)						x(G)			
Thuja-2,4(10)-diene	x(R)	x(n)									
α-Phellandrene	x(R)	x(n)	x(f)		x(x)						
β-Phellandrene					x(x)						
p-Cymene	x(R)	x(n)					x(D)				
Limonene	x(R)		x(f)		x(x)		x(D)	x(G)			
Linalool	x(R)		x(f)					x(G)			
α-Isocomene	x(R)				x(x)						
Methyl eugenol	x(R)										
Caryophyllene	x(R)		x(f)					x(G)			

Table 3 (*Continued*)

Compounds	*A. montana*	*S. trilobata*	*S. chilensis*	*C. uniflora*	*P. ruderale*	*C. nutans*	*P. brasiliensis*	*L. ericoides*	*L. salicifolia*	*L. pinaster*	*L. diamantinana*
Sesquiterpenes											
Eugenol	x(R)										
(*Z*)-β-Farnesene	x(R)		x(f)								
α-Humulene	x(R)		x(f)								
Germacrene D	x(R)		x(f)				x(E)				
α-Muurolene	x(R)										
γ-Cadinene	x(R)		x(f)								
δ-Amorphene	x(R)										
β-Sesquiphellandrene	x(R)										
cis-Sesquisabinene hydrate	x(R)										
Spathulenol	x(R)		x(f)		x(w)		x(D)				
Salvial-4(14)-isso-1-one	x(R)										
Humulene epoxide ii	x(R)										
α-Cadinol	x(R)										
epi-β-Bisabolol <	x(R)										
Cadalene	x(R)										
α-Bisabolol	x(R)										
Curcumene								x(G)			
Turmerol								x(G)			
Dihydro-ar-turmerone								x(G)			
α-Eudesmol			x(f)								
Diidroeudesmol			x(f)								
Caryophyllene			x(f)				x(D)				
Nerolidol			x(f)								
Sesquiterpene lactones											
Helenalin	x(Q,P)		x(g)								
Helenalin methacrylate	x(Q)										
6-*O*-isobutyril-tetrahydrohelenalin	x(Q)										
Helenalin acetate	x(Q)										
11,13-dihydrohelenalin	x(Q)		x(g)								
Arnicolide D	x(Q)										
Wedelolactone		x(o)									
Paludolactone		x(o)									
Trilobolide-6-*O*-isobutyrate		x (p)									
Triloboide-6-*O*-angelate		x(p)									
Triloboide-6-*O*-methacrylate		x(p)									
Oxidoisotrilobolide-6-*O*-isobutyrate		x(p)									
Oxidoisotrilobolide-6-*O*-methacrylate		x(p)									
Oxidoisotrilobolide-6-*O*-angelate		x(p)									
Wedeloide A		x(p)									
Wedeloide B		x(p)									
Desacetileupaserrine				x(r)							
2-α-Hydroxy-δβ-2′,3′,5′-trihydroxy-angeloyloxycostunolíde				x(r)							
2-α-hydroxy-δβ-3′-hydroxy-2′5′-epoxiangeloyloxy-costunolide				x(r)							
Ovatifolin				x(r)							
Crisanine							x(D)				
2′,3′-epoxy-15-deoxygoyazensolide								x(G)			
Dihydroeremantholide A								x(G)			

Table 3 (*Continued*)

Compounds	*A. montana*	*S. trilobata*	*S. chilensis*	*C. uniflora*	*P. ruderale*	*C. nutans*	*P. brasiliensis*	*L. ericoides*	*L. salicifolia*	*L. pinaster*	*L. diamantinana*
Eremantholide A								x(G)			
15-Desoxygoyazensolide								x(G)			
15-Acetoxygoyazensolide											x(G)
Goyazensolid								x(G)			
(4*S*,6*R*,7*S*,8*S*,10*R*,11*S*)-1-oxo-3,10-epoxy-8-angeloyloxygermacra-2-en-6(12)-olide								x(I)			
2′,3′-dihydro-15-deoxygoyazensolide								x(G)			
Lychnopholide								x(G)			
Lychnophorolide B								x(G)			
Costenolide									x(G)		
Eremanthin									x(G)		
Furanoheliangolyde										x(G)	
Goyazensolide											x(G)
15-Acetoxycentratherin											x(G)
Entraterine											x(G)
Diterpenes											
Xylopic acid		x(q)									
Solidagenone			x(h)								
Deoxysolidagenone			x(h)								
trans-Sabinol		x(p)									
ent-Kaur-16-em 19-oic acid (kaurenoic acid)		x(p)					x(D)				
3α-Cinnamoyloxykaur-16-*isso*-19-oic acid		x(p)									
3α-Tigloyloxykaur-16-*isso*-19-oic acid		x(p)									
ent-Kaur-9(11),dien-19-oic acid (grandiflorenic acid)		x(p)									
ent-Kaur-15-isso-19-oic acid (iso kaurenoic acid)		x(p)									
(3α)-3-(Angeloyloxy)-ent-kaur-16-em-19-oic acid		x(p)									
3α-(Angeloyloxy) 9β-hydroxy-ent-kaur-16en-19-oic acid		x(p)									

Table 3 (*Continued*)

Compounds	*A. montana*	*S. trilobata*	*S. chilensis*	*C. uniflora*	*P. ruderale*	*C. nutans*	*P. brasiliensis*	*L. ericoides*	*L. salicifolia*	*L. pinaster*	*L. diamantinana*
Triterpenes											
Lupeol									x(G)	x(M)	
Lupeol acetate									x(G)	x(M)	
Lupanol acetate									x(G)		
Friedelin										x(M)	
Acetyl lychnopholic acid								x(G)	x(G)	x(M)	x(G)
α-Amirine							x(D)	x(G)	x(G)	x(M)	
α-Amirine acetate							x(D)		x(G)	x(M)	
β-Amirine							x(D)	x(G)	x(G)	x(M)	
β-Amirine acetate							x(D)		x(G)	x(M)	
Pseudotaraxasterol							x(D)				
3-*O*-Acetyl-pseudotaraxasterol										x(M)	
Taraxasterol							x(D)				
15-Acetoxycentratherin											x(G)
Entratherin											x(G)
Phytosteroids											
4,4-Dimethyl-cholesta-22,24-dien-5-ol										x(G)	
Stigmasterol		x(k)								x(G)	
Sitosterol										x(G)	
**Thiophene derivatives*											
5-Methyl-2,2′:5′,2″-terthiophene					x(y)						
5′-Methyl-[5-(4-acetoxy-1-butynyl)]-2,2′-bithiophene					x(y)						
2,2′:5′,2″-Terthiophene					x(z)						
5-(But-1-yn-1-yl)-2,2′-bithiophene					x(z)						
Cyanogenic glycoside											
Prunasin						x					
Others											
Acetophenone			x(h)								
3-Methoxybenzaldehyde			x(i)								
Tetrachyrin			x(i)								
Farnesyl acetate	x(R)										
Methyl linoleate	x(R)										
Cubebin								x(G)			
Methylclusin								x(G)			
Yatein								x(G)			
α-Methylcubebin								x(G)			
Hinokinin								x(G)			
Lychnopholic acid								x (G)	x (G)	x (G)	x(G)
Acetyl lychnopholic acid								x (G)	x (G)	x (G)	x(G)

References: (a) Freires et al., 2010; (b) Gastaldi et al., 2018; (c) Tamura et al., 2009; (d) Sabir et al., 2012; (e) Schmeda-Hirschmann et al., 2002; (f) Marin, 2014; (g) Prudêncio, 2012; (h) Vechia et al., 2016; (k) Carvalho et al., 2001; (l) Lang et al., 2017; (m) Cechinel-Filho et al., 2004; (n) Verma et al., 2013; (o) Cechinel-Filho et al., 1997; (q) Batista et al., 2010; (r) Lima et al., 2015; (s) Lima et al., 2017; (t) Nascimento et al., 2007; (u) Wildner, 2016; (v) Fonseca et al., 2006; (x) Guillet et al., 1998; (y) Takahashi et al., 2011; (w) Raggi, 2013; (z) Lima-Neto, 1996; (A) Badilla et al., 1999; (B) Truiti et al., 2003 (C) Almeida et al., 2017; (D) Amorim et al., 2016; (E) Bohlmann et al., 1984; (F) Gobbo-Neto et al., 2005; (G) Semir et al., 2011; (H) Borella et al., 1998; (I) Sakamoto et al., 2003; (J) Gouvea et al., 2012; (K) Silva et al., 2013; (L) Ferreira et al., 2005; (M) Abreu et al., 2011; (N) Alfredo et al., 2008; (O) Nascimento et al., 2007; (P) Brazil, 2010; (Q) Marques, 2006; (R) Kowalski et al., 2015.

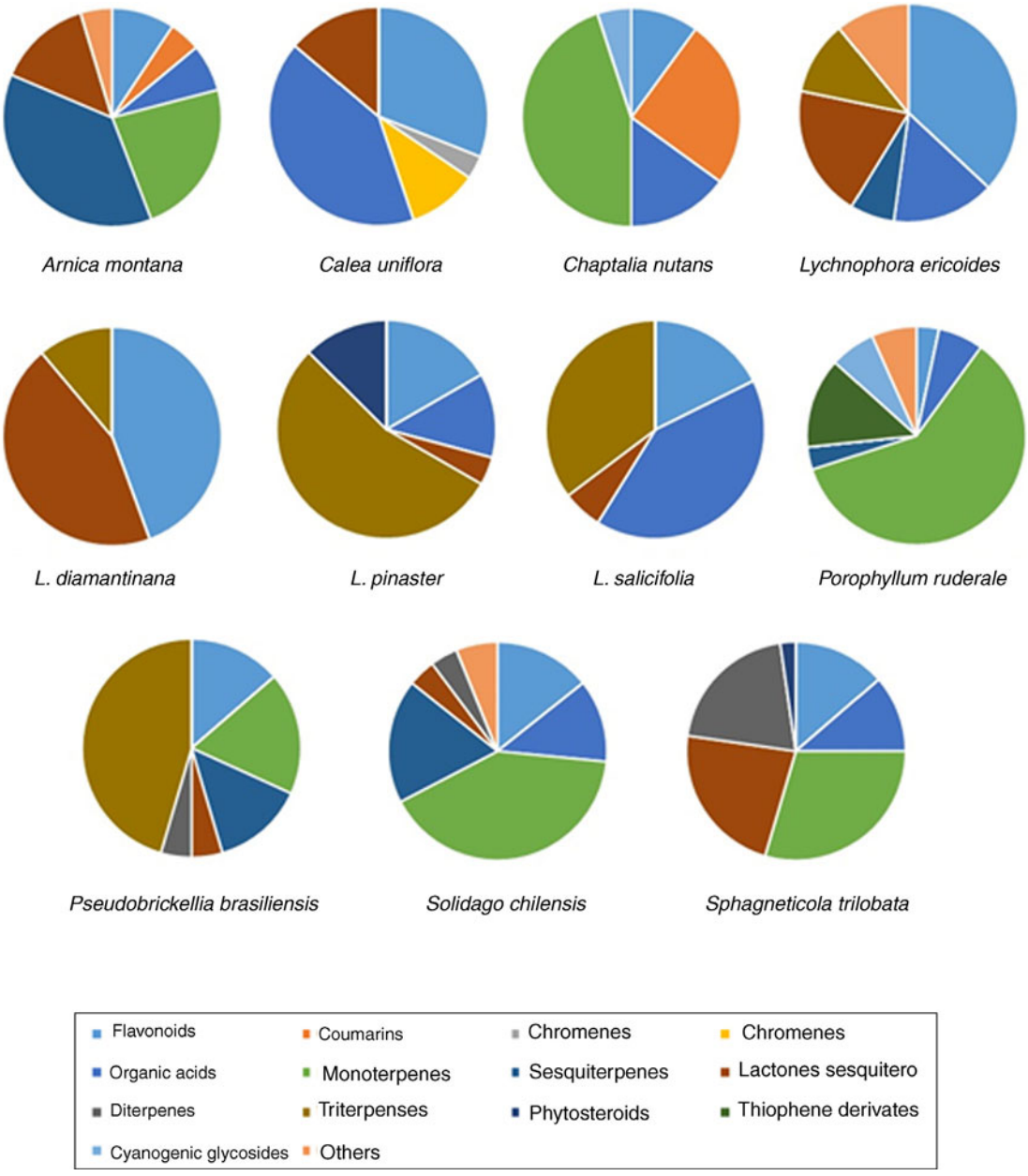

Fig. 21. Main classes of metabolites reported in each of the "arnicas" used in Brazil.

To the *S. chilensis*, a high concentration of starch grains was confirmed by the lugol test in the intermediary region of mesophyll (IR) of mesophyll. In this taxa, the presence of druses in the MV region is still observed. A study by Souza et al. (2017) evaluating this species, described the presence of several calcium oxalate crystals in the forms of raphides, prismatic crystals and druses, however, this was not observed in this work. *S. trilobata* presented druses in the MV region. According to Baccarin et al. (2009), calcium oxalate crystals (several druses and some prismatic crystals) were found only in the stem section, so there was no description of their presence in the leaves of *S. trilobata* before the present work. The presence of small druses is remarkable in the species *L. diamantinana*, in every region of the mesophyll. In the other species of *Lychnophora* no crystals were observed. In *P. brasiliensis* and *P. ruderale* the presence of crystals was also not observed.

According to the Brazilian Phamacopea 5 ed. (Farmacopeia Brasileira, 2010), *A. montana* (flowers) presents characteristics quite different from those observed in Brazilian "arnica" species, as in cross section. It is described the occurrence of non-glandular trichomes of different types: uniseriate and multicellular, formed by 4 or 5 cells and different sizes and uniseriate and multicellular non-glandular trichomes, consisting of 1–3 proximal cells with thickened walls and 2–4 distal thin-walled cells. Glandular trichomes of unicular and multicellular pedicel, unicellular and capitate; biseriate and pluricellular pedicel. Anomocytic stomata. The bracts presents fundamental parenchyma, with vascular bundles corresponding to the middle vein. The receptacle, in cross section, also shows fundamental parenchyma, with vascular bundles and secretory channels. The corolla of the ligated flower, in frontal view, presents epidermis of the adaxial face with cells of

polygonal, papillary and anticline. The epidermis of the abaxial face presents cells of anticlinal walls elongated, almost straight, but undulating in the distal portion. In this way, the *A. montana* microanatomic identification must comply with the official compendia as, Pharmacopoea.

Histochemical analyses

The histochemical analyses carried out for the ten species of "arnicas" confirm the presence of chemical classes related to important chemotaxonomic markers for the Asteraceae family (Keles et al., 2011). Among them, general phenolic compounds and terpenoids, including sesquiterpene lactones. The histochemical analyses performed in this study indicate the glandular trichomes as the main site of synthesis and accumulation of chemotaxonomic markers. However, we also observed other sites of synthesis/accumulation of the evaluated compounds, as the epidermal idioblasts and parenchyma tissues in the fully expanded leaves, as it was already described by Lusa et al. (2016a,b). In all the secretory structures identified, the secreted content can be considered mixed, by the presence of more than one group of substances, which are generally accumulated at the same time, also according to descriptions of Lusa et al. (2016a,b).

The indicative histochemical reaction for sesquiterpene lactones also points to glandular trichomes as the main site of synthesis and accumulation of these substances. This data is in agreement with Spring et al. (2001) that indicates the glandular trichomes as main sites of synthesis and accumulation of sesquiterpene lactones in species of the family. However, the histochemical indication of general terpenoids accumulated in cells of parenchyma tissues (leaves) may be related to the possible presence of lactones in glabrous leaf species such as the species *P. ruderale* and *P. brasiliensis*. Among the secondary metabolites present in Asteraceae, terpenoids (mono, sesqui, di and triterpenes and sesquiterpene lactones) and phenolic compounds (flavonoids and cinnamic acid derivatives) are the most representative classes of substances and are considered important chemotaxonomic markers due to its enormous chemical variety (Lima et al., 2015).

Phytochemical review

The phytochemical review showed different chemotaxonomic markers for the species. The most abundant metabolite classes described for the species, respectively, are terpenes (mono and sesquiterpenes) for *A. montana*; derivatives of organic acids, sesquiterpene lactones and flavonoids for *S. trilobata* (Cechinel-Filho et al., 2004; Lang et al., 2017); terpenes (monoterpenes and sesquiterpenes, including sesquiterpene lactones), flavonoids and organic acid derivatives for *S. chilensis* (Freires et al., 2010; Souza et al., 2017); derivatives of phenolic acids, flavonoids, chromenes and chromanones in *C. uniflora* (Lima et al., 2015); monoterpenes in *P. ruderale* (Fonseca et al., 2006); monoterpenes and coumarins in *C. nutans* (Gastaldi et al., 2018); triterpenes, monoterpenes and flavonoids in *P. brasiliensis* (Tamura et al., 2009). For species of the genus *Lychnophora*, flavonoids, organic acid derivatives, sesquiterpene lactones and triterpenes were observed (Semir et al., 2011).

Some similarities and differences between species can be verified, as the presence of flavonoids such as the chalcone pinostrobin and the flavone crisin in the species *L. ericoides*, *L. diamantinana*, *L. salicifolia* and *L. pinaster* (Semir et al., 2011). The flavone quercitin and the flavonol patuletin are present in *S. chilensis* and *A. montana* (Valverde et al., 2012; Marin, 2014). The chalcone butein was reported for *C. uniflora* (Lima et al., 2017), and methoxyflavones in *S. trilobata* (Lang et al., 2017). The presence of the ubiquitous phenolic acids quinic, caffeic and feluric are described in all the species of "arnicas" studied (Empinotti and Duarte, 2006; Semir et al., 2011; Marin, 2014; Lima et al., 2017; Lusa et al., 2016a,b; Lang et al., 2017).

Lipophilic substances include terpenes, free fatty acids, flavonoid aglycons, waxes, essential oils, among others. The presence of sesquiterpene lactones and diterpenes in the "arnicas" are described as chemical markers such as the sesquiterpene lactone helenalin present in *A. montana* (Farmacopeia Brasileira, 2010). Another example is the presence of diterpene solidagenone in *S. chilensis*, used as a marker for quality control of the plant drug (Valverde et al., 2012).

Phytochemical studies with species of the Vernonieae tribe address the predominance of sesquiterpenes (66%) (Keles et al., 2011). Through the compilation of several authors by Semir et al. (2011) reported a large concentration of sesquiterpenes in the genus *Lychnophora*, including the species *L. ericoides*, *L. diamantinana*, *L. salicifolia* and *L. pinaster*, with emphasis on sesquiterpene lactones.

S. trilobata presents a high concentration of monoterpenes, diterpenes and sesquiterpenes, for example, the sesquiterpene lactone paludolactone and the wedeloides A and B (Lang et al., 2017). The *C. uniflora* is known for the presence of substances with lipophilic characteristics, namely the sesquiterpene lactones desacethyleupaserrin and ovatifolin (Lima et al., 2017). The species is rich in flavonoids, chromenes and phenolic acids. The arnica *P. ruderale* presents expressive amount of monoterpenes as α-pinene, mircene, limonene among others. For *C. nutans* there are not many literatures referring to the chemical profile of the plant, in these the presence of polyphenols and flavonoids, coumarins, cyanogenic glucosides is observed (Badilla et al., 1999; Truiti et al., 2003). Generally, a review by Chadwick et al. (2013) have pointed out that sesquiterpenoids, specifically the sesquiterpene lactones of Asteraceae, may play a significant role in human health due to their potential for the treatment of various pathologies, in addition to being related to plant metabolism against exogenous predators.

Conclusions

The information about plant morphology, histology and secondary metabolites in plants are some of the fundamental factors that support the chemical investigations of the species, since there are still few studies that show which are the structures responsible for the production of chemotaxonomic markers as well as occurrence sites in species and/or genera. In view of the use of these species of "arnica" with medicinal purpose in Brazil and the little knowledge about the chemotaxonomy and scientific evidence of its therapeutic potentials it is relevant to investigate, besides morphological and anatomical aspects of the species, the chemical profile of the extracts of these plants from traditional preparations.

Ethical disclosures

Protection of human and animal subjects. The authors declare that no experiments were performed on humans or animals for this study.

Confidentiality of data. The authors declare that they have followed the protocols of their work center on the publication of patient data.

Right to privacy and informed consent. The authors declare that no patient data appear in this article.

Authors' contributions

AEA collected the plants, carried out the anatomical analysis and wrote the manuscript. ER and JW performed the anatomical analysis. MGL and MWB created the project and supervised the laboratory work. All the authors have read the final manuscript and approved the submission.

Conflicts of interest

The authors declare no conflicts of interest.

Acknowledgments

Our thanks to the Laboratory of Plant Anatomy, Botany Department of the Biological Sciences Center of the Federal University of Santa Catarina (UFSC) for granting the space and materials available. Central Laboratory of Electronic Microscopy of the UFSC to SEM analyses. Thanks to FLOR Herbarium and Didactic Horto of Medicinal Plants of the Health Sciences Center of the UFSC to available some vegetal samples used. Thanks to Rafael Trevisan and Pedro Fiaschi for assisting in the identification of plant species and thanks to Benoit Francis Patrice Loeuille to available to the *Lychnophora* samples used.

Appendix A. Supplementary data

Supplementary data associated with this article can be found, in the online version, at doi:10.1016/j.bjp.2019.02.006.

References

Abreu, V.C.G., Takahashi, J.A., Duarte, L.P., Piló-Veloso, D., Junior, P.A.S., Alves, D., Romanha, A.J., Alcântara, A.F., 2011. Evaluation of the bactericidal and trypanocidal activities of triterpenes isolated from the leaves, stems, and flowers of *Lychnophora pinaster*. Rev. Bras. Farmacogn. 21, 615–621.

Alfredo, P.P., Anaruma, C.A., Pião, A.C.S., João, S.M.A., Casarotto, R.A., 2008. Qualitative analysis of effects of phonophoresis with *Arnica montana* onto acute inflammatory process in rat skeletal muscles. Fisioter. Pesqui. 15, 273–279.

Almeida, V.G., Avelar-Freitas, B.A., Santos, M.G., Costa, L.A., Silva, T.J., Pereira, W.F., Amorim, M.L.L., Grael, C.F.F., Gregório, L.E., Rochavieira, E., Brito-Mel, G.E.A., 2017. Inhibitory effect of the *Pseudobrickellia brasiliensis* (Spreng) R.M King & H. Rob. aqueous extract on human lymphocyte proliferation and IFN-γ and TNF-α production in vitro. Braz. J. Med. Biol. Res. 50, 1–8.

Amorim, M.L.L., Godinho, W.M., Archanjo, F.C., Grael, C.F.F., 2016. Chemical constituents of *Pseudobrickellia brasiliensis* leaves (Spreng.) R.M. King & H. Rob. (Asteraceae). Rev. Bras. Plantas Med. 18, 408–414.

Baccarin, T., Czepula, A.I., Ferreira, R.A., Lucinda, R.M., 2009. Análise morfoanatômica das partes aéreas de *Wedelia paludosa* DC. (*Acmela brasiliensis*, *Sphagneticola trilobata*), Asteraceae. Rev. Bras. Farmacogn. 19, 612–616.

Badilla, B., Mora, G., Poveda, L.J., 1999. Antiinflammatory activity of aqueous extracts of five Costa Rican medicinal plants in Sprague-Dawley rats. Rev. Biol. Trop. 47, 723–727.

Batista, R., García, P.A., Castro, M.A., Corral, J.M., Feliciano, A., Oliveira, A., 2010. Iso-Kaurenoic acid from *Wedelia paludosa* D.C. An. Acad. Bras. Cienc. 82, 823–831.

Bohlmann, F., Zdero, C., King, R.M., Robinson, H., 1984. A hydroxygermacrene and other constituents from *Pseudobrickellia brasiliensis*. Phytochemistry 23, 1798–1799.

Borella, J.C., Lopes, J.L., Vichnewski, W., Cunha, W.R., Herz, W., 1998. Sesquiterpene lactones, triterpenes and flavones from *Lychnophora ericoides* and *Lychnophora pseudovillosissima*. Biochem. Syst. Ecol. 26, 671–676.

Brazil, 2010. Farmacopéia Brasileira, 5ª ed. Agência Nacional de Vigilância Sanitária, Brasília, pp. 546.

Budel, J.M., Duarte, M.R., Farago, P.V., Takeda, I.J.M., 2006. Caracteres anatômicos de folha e caule de *Calea uniflora* Less., Asteraceae. Rev. Bras. Farmacogn. 16, 53–60.

Carvalho, G.J.A., Carvalho, M.G., Ferreira, D.T., Faria, T.J., Braz-Filho, R., 2001. Diterpenos, triterpenos e esteróides das flores de *Wedelia paludosa*. Quim. Nova 24, 24–26.

Cechinel-Filho, V., Block, L.C., Yunes, R.A., Monache, F.D., 2004. Paludolactone: A new Eudesmanolide Lactone from Wedelia Paludosa Dc. (Acmela Brasiliensis). Nat. Prod. Res. 18, 47–451.

Chadwick, M., Trewin, H., Gawthrop, F., Wagstaff, C., 2013. Sesquiterpenoids lactones: benefits to plants and people. Int. J. Mol. Sci. 14, 12780–12805.

Duarte, M.R., Siebenrok, M.C.N., Empinotti, C.B., 2007. Anatomia comparada de espécies de arnica: *Porophyllum ruderale* (Jacq.) Cass. e *Chaptalia nutans* (L.) Pohl Rev. Cienc. Farm. Basica Apl. 28, 193–201.

Empinotti, C.B., Duarte, M.R., 2006. Caracteres anatômicos de arnica-do-campo: *Chaptalia nutans*. Acta Farm. Bonaer. 25, 333–338.

Fernandes, Y.S., Trindade, L.M.P., Rezende, M.H., Paula, J.R., Gonçalves, L.A., 2016. Trichomes and chemical composition of the volatile oil of *Trichogonia cinerea* (Gardner) R.M. King & H. Rob. (Eupatorieae Asteraceae). An. Acad. Bras. Cienc. 88, 309–322.

Ferreira, A.A., Azevedo, A.O., Silveira, D., Oliveira, P.M., Castro, M.S.A., Raslan, D.S., 2005. Constituents of *Lychnophora pinaster* hydroalcoholic extract. Chem. Nat. Comp. 41, 466.

Fonseca, M.C.M., Meira, R.M.S.A., Casali, V.W.D., 2006. Anatomia dos órgãos vegetativos e histolocalização de compostos fenólicos e lipídicos em *Porophyllum ruderale* (Asteraceae). Planta Daninha 24, 707–713.

Freires, I.A., Alves, L.A., Jovito, V.C., Almeida, L.F.D., Castro, R.D., Padilha, W.W.N., 2010. In vitro antibacterial and antiadherent activities of tinctures from *Schinus terebinthifolius* (Aroeira) and *Solidago microglossa* (Arnica) on dental biofilm forming bacteria. Odontol. Clín.-Cient. 9, 139–143.

Gastaldi, B., Catalán, C.A., Silva-sofrás, F.M., González, S.B., 2018. *Solidago chilensis* Meyen (Asteraceae), a medicinal plant from South America. A comprehensive review: ethnomedicinal uses, phytochemistry and bioactivity. B. Latinoam. Caribe Pl. 17., pp. 17–29.

Geissman, T.A., Griffin, T.S., 1971. Sesquiterpene lactones: acid-catalyzed color reactions as an aid in structure determination. Phytochemistry 10, 2475–2485.

Gobbo-Neto, L., Santos, M.D., Kanashiro, A., Almeida, M.C., Lucisano-Valim, Y.M., Lopes, J.L.C., Souza, G.E.P., Lopes, N.P., 2005. Evaluation of the anti-Inflammatory and antioxidant Activities of di-*C*-glucosylflavones from *Lychnophora ericoides* (Asteraceae). Planta Med. 71, 3–6.

Gouvea, D.R., Meloni, F., Ribeiro, A.B.B., Lopes, J.L.C., Lopes, N.P., 2012. A new HPLC-DAD-MS/MS method for the simultaneous determination of major compounds in the crude extract of *Lychnophora salicifolia* Mart. (Brazilian arnicão) leaves: application to chemical variability evaluation. Anal. Chim. Acta 748, 28–36.

Guillet, G., BełLanger, A., Arnason, J.T., 1998. Volatile monoterpenes in *Porophyllum gracile* and *P. ruderale* (Asteraceae): identification, localization and insecticidal synergism with α-terthienyl. Phytochemistry 49, 423–429.

Jensen, W.A., 1962. Botanical Histochemistry (Principles and Pratice). W.H. Freeman and Company, San Francisco.

Johansen, D.A., 1940. Plant Microtechnique. Mc Graw Hill Book, New York.

Keles, L.C., Gianasi, F.M., Souza, R.C., Brito, B.L., Schaab, E.H., Souza, M.G.M., Carvalho, T.C., Martins, C.H.G., Veneziani, R.C.S., Cunha, W.R., Crotti, A.E.M., 2011. Antibacterial activity of 15-deoxygoyazensolide isolated from the stems of *Minasia alpestris* (Asteraceae) against oral pathogens. Nat. Prod. Res. 25, 326–331.

Kowalski, R., Sugier, D., Sugier, P., Kolodzij, B., 2015. Evaluation of the chemical composition of essential oils with respect to the maturity of flower heads of *Arnica montana* L. and *Arnica chamissonis* Less. cultivated for industry. Ind. Crop. Prod. 76, 857–865.

Lang, K., Corrêa, J., Wolff, F., Da Silva, G.F., Malheiros, A., Filho, V.C., Silva, R.M.L., Quintão, N.L.M., Sandjo, L.P., Bonomini, T.J., Bresolin, T.M.B., 2017. Biomonitored UHPLC-ESI-QTOF-MS and HPLC-UV thermostability study of the aerial parts of *Sphagneticola trilobata* (L.) Pruski, Asteraceae. Talanta 167, 302–309.

Lima, T.C., Souza, R.J., Moraes, M.H., Steindel, M., Biavatti, M.W., 2017. New furanoheliangolide sesquiterpene lactone from *Calea pinnatifida* (R Br.) Less. (Asteraceae) and evaluation of its trypanocidal and leishmanicidal activities. J. Braz. Chem. Soc. 28, 367–375.

Lima, T.C., Souza, R.J., Santos, A.D.C., Moraes, M.H., Biondo, N.E., Barison, A., Steindel, M., Biavatti, M.W., 2015. Evaluation of leishmanicidal and trypanocidal activities of phenolic compounds from *Calea uniflora* Less. Nat. Prod. Res. 30, 551–557.

Lima-Neto, D.A. Estudo fitoquímico e efeitos analgésicos da *Porophyllum ruderale*, 1996. PhD thesis, Curso de Farmacologia, Universidade Estadual de Campinas, Piracicaba.

Lusa, M.G., Costa, F.B., Appezzato-da-Gloria, B., 2016a. Histolocalization of chemotaxonomic markers in Brazilian *Vernonieae* (Asteraceae). Bot. J. Linn. Soc. 182, 581–593.

Lusa, M.G., Martucci, M.E.P., Loeuille, B.F.P., Gobbo-Neto, L., Appezzato-da-Glória, B., Costa, F.B., 2016b. Characterization and evolution of secondary metabolites in Brazilian Vernonieae (Asteraceae) assessed by LC–MS fingerprinting. Bot. J. Linn. Soc. 182, 594–661.

Marin, R., 2014. *Solidago chilensis* Meyer: desenvolvimento de métodos analíticos, extratos secos qualificados, avaliação farmacológica in vivo e produção de comprimidos. PhD Thesis, Programa em Ciencias Farmaceuticas, Universidade Federal do Rio Grande do Sul, Porto Alegre.

Marques, M., 2006. Estudo da resposta imunológica induzida por *Arnica montana* L. PhD Thesis. Programa em Ciências Farmacêuticas, Biociências e Biotecnologia Aplicadas à Farmácia, Universidade Estadual Paulista, Araraquara.

Metcalfe, C.R., Chalk, L., 1988. Anatomy of Dicotyledons, 2nd ed. Clarendon Press. US, Oxford.

Milan, P., Hayashi, A.H., Appezzato-da-Glória, B., 2006. Comparative leaf morphology and anatomy of three Asteraceae species. Braz. Arch. Biol. Techn. 49, 135–144.

Nascimento, A.M., Costa, F.C., Thiemann, O.H., Oliveira, D.C.R., 2007. Chromanones with leishmanicidal activity from *Calea uniflora*. Z. Naturforsch. C. 62, 353–356.

Obón, C., Rivera, D., Verde, A., Fajardo, J., Valdes, A., Alcaraz, F., Carvalho, A.M.M., 2012. *Arnica*: a multivariate analysis of the botany and ethnopharmacology of a medicinal plant complex in the Iberian Peninsula and the Balearic Islands. J. Ethnopharmacol. 144, 44–56.

Prudêncio, R., 2012. Levantamento etnofarmacológico de *Solidago chilensis* Meyen. "Arnica-brasileira" (Asteraceae). Especialista em Ecologia e Manejo de Recursos Naturais, Universidade do Extremo Sul Catarinense, Criciúma.

Raggi, L., 2013. Teor, composição química e atividade biológica de óleos voláteis de *Sphagneticola trilobata* (L.) Pruski e *Porophyllum ruderale* (Jacq.) Cass. (Asteraceae). PhD Thesis, Programa – Biodiversidade Vegetal e Meio Ambiente, Área de Concentração de Plantas Vasculares em Análises Ambientais, Instituto de Botânica da Secretaria do Meio Ambiente.

Rodríguez-Chávez, J.L., Egas, V., Linares, E., Bye, R., Hernández, T., Espinosa-García, F.J., Delgado, G., 2017. Mexican arnica (*Heterotheca inuloides* Cass Asteraceae: Astereae). J. Ethnopharmacol. 195, 39–63.

Sabir, S.M., Ahmad, S.D., Hamid, A., Khan, M.Q., Athayde, M.L., Santos, D.B., Boligon, A.A., Rocha, J.B.T., 2012. Antioxidant and hepatoprotective activity of ethanolic extract of leaves of Solidago microglossa containing polyphenolic compounds. Food Chem. 131, 741–747.

Sakai, W.S., 1973. Simple method for differential staining of paraffinn embedded -plant material using toluidine blue. Stain Technol. 43, 247–249.

Sakamoto, H.T., Flausino, D., Castellano, E.E., Stark, C.B.W., Gates, P.J., Lopes, N.P., 2003. Sesquiterpene lactones from *Lychnophora ericoides*. J. Nat. Prod. 66, 695–963.

Sales, M.D.C., Sartor, E.B., Gentilli, R.M., 2015. Ethnobotany and ethnopharmacology: traditional medicine and the bioprospection of phytotherapics. Salus J. Res. Health Sci. 1, 17–25.

Sandini, T.M., Udo, M.S.B., Spinosa, H.S., 2013. *Senecio brasiliensis* e alcaloides pirrolizidínicos: toxicidade em animais e na saúde humana. Biotemas 26, 83–92.

Schmeda-Hirschmann, G., Rodriguez, J., Astudillo, L., 2002. Gastroprotective activity of the diterpene solidagenone and its derivatives on experimentally induced gastric lesions in mice. J. Ethnopharmacol. 81, 111–115.

Semir, J., Rezende, A.R., Monge, M., Lopes, N.P., 2011. As arnicas endêmicas das serras do Brasil: Uma revisão sobre a biologia e a química das espécies de *Lychnophora* (Asteraceae), 1st ed. UFOP, Ouro Preto, MG.

Silva, P.S.S., Linhares, J.F.P., Marques, M.O.M., 2013. Caracterização morfológica, perfil químico, atividade biológica e conservação in situ do gênero *Lychnophora* Mart. (Asteraceae: Vernonieae: Lychnophorinae), Brasil. Biotemas 26, 201–203.

Smith, F.H., Smith, E.C., 1942. Anatomy of the inferior ovary of *Darbya*. Am. J. Bot. 29, 464–471.

Souza, D.M.F., Souza, R.D., Sá, E.L., Araújo, Randau, K.P., 2017. Anatomical, phytochemical and histochemical study of *Solidago chilensis* Meyen. An. Acad. Bras. Cienc. 90, 2107–2120.

Spring, O., Zipper, R., Reeb, S., Vogler, B., Da Costa, F.B., 2001. Sesquiterpene lactones and a myoinositol from glandular trichomes of *Viguiera quinqueremis* (Heliantheae; Asteraceae). Phytochemistry 57, 267–272.

Takahashi, H.T., Novello, C.R., Ueda-Nakamura, T., Dias Filho, B.P., Palazzo De Mello, J.C., Nakamura, C.V., 2011. Thiophene derivatives with antileishmanial activity isolated from aerial parts of *Porophyllum ruderale* (Jacq.) Cass. Molecules 16, 3469–3478.

Tamura, E.K., Jimenez, R.S., Waismam, K., Gobbo-Neto, L., Lopes, N.P., Malpezzi-Marinho, E.A.L., Marinho, E.A.V., Farsky, S.H.P., 2009. Inhibitory effects of *Solidago chilensis* Meyen hydroalcoholic extract on acute inflammation. J. Ethnopharmacol. 122, 478–485.

Truiti, M.C.T., Sarragiotto, M.H., Filho, B.A.A., Nakamura, C.V., Dias Filho, B.P., 2003. In vitro antibacterial activity of a 7-*O*-β-D-glucopyranosyl-nutanocouMarin from *Chaptalia nutans* (Asteraceae). Mem. I. Oswaldo Cruz 98, 283–286.

Valverde, S.S., Oliveira, T.B., Souza, S.P., 2012. *Solidago chilensis* Meyen (Asteraceae). Rev. Fitos 7, 131–136.

Vechia, C.A.D., Morais, B., Schonell, A.P., Diel, K.A.P., Faust, C., Menin, C., Gomes, D.B., Roman Junior, W.A., 2016. Isolamento químico e validação analítica por cromatografia líquida de alta eficiência de quercitrina em *Solidago chilensis* Meyen (Asteraceae). Rev. Bras. Pl. Med. 18, 288–296.

Verma, R.S., Padalia, R.C., Chauhan, A., Sundaresan, V., 2013. Essential oil composition of *Sphagneticola trilobata* (L.) Pruski from India. J. Essent. Oil Res. 26, 29–33.

Wildner, L.M., 2016. Atividade antimicobacteriana in vitro de lactonas sesquiterpênicas e investigação do seu mecanismo de ação. PhD Thesis. Programa de Pós-graduação em Farmácia, Universidade Federal de Santa Catarina. Florianópolis.